

Effects of Phonons and Nuclear Spins on the Tunneling of a Domain Wall

M. Dubé^{1,3,4} and P. C. E. Stamp^{1,2}

¹*Physics and Astronomy Department and* ²*Canadian Institute for Advanced Research,
University of British Columbia, 6224 Agricultural rd., Vancouver, BC, Canada V6T 1Z1*

³*Helsinki Institute of Physics, P.O. Box 9 (Siltavuorenpenger 20 C), FIN-00014,
University of Helsinki, Finland*

⁴*Laboratory of Physics, P.O. Box 1000, FIN-02150 HUT,
Helsinki University of Technology, Espoo, Finland*

We consider the quantum dynamics of a magnetic domain wall at low temperatures, where dissipative couplings to magnons and electrons are very small. The wall motion is then determined by its coupling to phonons and nuclear spins, and any pinning potentials.

In the absence of nuclear spins there is a dominant superOhmic 1-phonon coupling to the wall *velocity*, plus a strongly T -dependent Ohmic coupling to pairs of phonons. There is also a T -independent Ohmic coupling between single phonons and the wall chirality, which suppresses “chirality tunneling”. We calculate the effect of these couplings on the T -dependent tunneling rate of a wall out of a pinning potential.

Nuclear spins have a very strong and hitherto unsuspected influence on domain wall dynamics, coming from a hyperfine-mediated coupling to the domain wall position. For $k_B T \gg \omega_0$ this coupling yields a spatially random potential, fluctuating at a rate governed by the nuclear T_2 . When $k_B T \ll \omega_0$, the hyperfine potential fluctuates around a *linear* binding potential.

The wall dynamics is influenced by the fluctuations of this potential, i.e., by the nuclear spin dynamics. Wall tunneling can occur when fluctuations open an occasional “tunneling window”. This changes the crossover to tunneling and also causes a slow “wandering”, in time, of the energy levels associated with domain wall motion inside the pinning potential. This effect is fairly weak in Ni - and Fe - based magnets, and we give an approximate treatment of its effect on the tunneling dynamics, as well as a discussion of the relationship to recent domain wall tunneling experiments.

PACS numbers:

I. INTRODUCTION

The quantum dynamics of mesoscopic or even macroscopic magnetic solitons has been the subject of considerable interest in the last few years. There are several reasons for this. One is the rapid development of the new field of nanomagnetism¹, in which very small magnetic wires, films, and magnetic macromolecules² (as well as molecular chains) can be prepared. In many cases one expects that solitons such as domain walls, or perhaps lower-dimensional vortices and skyrmions, will play an important role in the quantum dynamics of nanomagnets at low temperatures in systems as diverse as magnetic perovskites, the cuprate superconductors, or nanomagnetic wires, films, and junctions. The magnetic dynamics also strongly influence the charge transport in some systems.

A second reason for this interest stems from the continued fascination with macroscopic quantum phenomena. Previously associated almost exclusively with superfluids and superconductors, it has become clear in recent years that magnetic systems may also exhibit macroscopic quantum phenomena^{3,4}, perhaps the most spectacular being the possible quantum tunneling of macroscopic domain walls in ferromagnets^{3,5}. There now exists some experimental support for tunneling of *single* domain walls in Ni wires⁶⁻⁹, as well as many earlier experiments on multi-wall systems¹⁰⁻¹². The tunneling dynamics of large flexible domain walls poses many interesting theoretical problems, particularly concerning the role played by the various environmental degrees of freedom, which couple to the wall in various ways.

This is the main subject of this paper, which deals with the hitherto neglected effects of phonons and nuclear spins on magnetic domain wall tunneling (a limited discussion of phonon effects was given previously^{3,5}, but was very incomplete). We find that the effect of the nuclear spins in particular can be quite spectacular, and can completely contradict the picture of quantum domain wall dynamics that has evolved over the last few years. We derive a new scenario, in which magnetic domain wall dynamics is influenced at low temperatures by the effective coupling of the wall to a random (in space) “hyperfine field”, which also fluctuates in time. Even in Ni wires (where these effects are far weaker than in other magnets), this fluctuating hyperfine field will be shown to have some influence on wall tunneling. The phonons are found to have a much weaker effect, but one nevertheless important to evaluate when one

considers the finite- T tunneling rate (particularly in isotopically purified systems, where phonons entirely determine the low- T dissipative dynamics, if the system is pure and insulating). We shall also see that phonons couple very strongly to the domain wall chirality, and thereby suppress chirality tunneling.

In the remainder of this section we give a brief explanation of previous work in this field, and note how the present paper fits into this.

A. Macroscopic Quantum Phenomena in Magnets

The history of macroscopic quantum phenomena goes back to the 1930's (Meissner effect, superfluid fountain effect, capillary superflow, etc), and has until recently been associated almost exclusively with superconductors and superfluids. In recent years considerable attention has focused on Caldeira and Leggett's proposal that SQUIDS and related systems might show macroscopic flux tunneling¹³. Subsequent experiments^{14–18} confirmed their work quantitatively, and this is still an active field¹⁹.

It is obviously important to find other systems in which quantum macroscopic phenomena occur. It should be stressed that this is not just a question of energetics but also involves the “environmental decoherence” which almost always destroys quantum phase correlations at all but the microscopic level. Consider, eg., the possibility of “macroscopic quantum tunneling” (MQT) just mentioned. Many authors have suggested MQT after having noted the existence of some small tunneling barrier acting on some large collective mode - there is a long list of candidates for such MQT. The list includes ^4He superfluid^{20,21} and ^3He superfluid²², superconductors^{13,23} ferroelectrics²⁴, charge density waves (CDW) tunneling in 1-dimensional systems²⁵, MQT and tunneling nucleation of dislocations, vacancies and impurities in quantum solids²⁶, quantum diffusion of such objects in quantum solids²⁷, as well as in normal²⁸ and superfluid²⁹ ^3He . To this list we may also add more general studies of quantum nucleation³⁰ as well as of large scale tunneling in cosmology³¹. This list is certainly not complete. Finally there are the various kinds of macroscopic quantum phenomena, including MQT, which have been suggested for magnetic systems, to which we come below.

Despite the length of this list, in few cases have these suggestions been confirmed by experiments. There are two main reasons for this. First, the the surrounding “quantum environment” usually strongly suppresses MQT (and completely suppresses “macroscopic quantum coherence” (MQT)). Consequently, as emphasised by Leggett et. al^{13,32–34} any discussion of MQT which ignores the environmental effects is usually of of academic interest only.

A second reason is simply that most physical materials contain defects, impurities and other imperfections. The coupling of these to the collective coordinates involved in MQT is often much larger than the very small tunneling barriers. Since such external effects are usually unknown, this makes experimental tests very difficult.

So far, the only case where really indisputable evidence can be given for the observation of MQT is in superconductors (in SQUIDS and other Josephson devices¹⁸). This work has been widely reviewed^{18,34}. In magnetic systems, suggestions that tunneling phenomena might exist go back over 40 years^{35,36}. These suggestions typically involved some 1-dimensional phenomenological potential (a “pinning potential” for domain walls, an anisotropy potential for monodomain grains) to which a naive WKB analysis was applied. No microscopic theory was attempted, and the experimental evidence lacked any clear theoretical basis.

However, the picture that has emerged in recent years is very different from this, for 2 main reasons. The first is the realisation that a standard WKB analysis is inappropriate to spin systems, in which a constraint typically exists - in small particles or macromolecules at low T the magnetisation density $|\mathbf{M}|$ is roughly constant (although not necessarily in domain walls, if multi-magnon excitations are important⁵). This constraint leads to a kinetic energy which is linear in time derivatives (not quadratic). Thus a correct solution for the problem of tunneling of a spin was not given until 1986, by van Hemmen and Suto^{37–39} (and independently for a particular case by Enz and Schilling⁴⁰). Both of these analyses were semi-classical. A key role in nanomagnetic dynamics is also played by the “Kramers/Haldane phase”, which differs for integer and half-integer spins; this has no analogue in superconductors^{38,41,42}.

The second reason for the revised picture is that once microscopic theories were attempted of domain wall tunneling, or of tunneling in nanomagnets, it became obvious that yet again, much of the physics was in the coupling to the background quantum environment. Some of this physics is very different from that in superconductors. In particular, the coupling to nuclear spins is very strong, can play a major role in controlling the quantum dynamics of mesoscopic or nanoscopic magnets, and cannot obviously be understood in terms of an “oscillator bath” model of the environment^{43–48}. Extensive theory has been done in an effort to understand the way in which the environment determines nanomagnetic dynamics, both in particles and molecules^{3,43,47,49,50} and in domain wall dynamics (see below).

Since this theoretical work was done, strong experimental evidence has emerged for tunneling phenomena in mesoscopic magnetic systems at low temperature. This includes many experiments on multi-grain systems⁵¹ and on systems with multiple domains⁵²; evidence has been claimed both for magnetisation tunneling in monodomain systems and for

domain wall tunneling in multi-domain systems. There has also been a claim for the observation of coherent tunneling in large ferritin molecules⁵³, which has been disputed by various authors⁵⁴. A very interesting set of experiments by Giordano et. al.⁶⁻⁹ reports strong evidence for tunneling of single domain walls in Ni wires, to which we will return below. Finally, a whole series of experiments on Mn₁₂-acetate molecular crystals gives strong evidence for thermally activated resonant tunneling in this system⁵⁵.

B. Domain Wall Tunneling

The principal results to emerge from the first microscopic analyses of domain wall tunneling have been:

(a) The effective pinning potential for a wall is almost independent of the nature of the pinning centre, provided the spatial extent of the pinning centre (usually some kind of defect) is much smaller than the wall width λ ; the shape of the defect is also not important in this case³. The pinning potential is of the form $V(Q) = -V_0 \text{sech}^2(Q/\lambda)$, where V_0 is positive. Subsequent analyses of the so-called “domain wall junction” rely on this result, which is important for any comparison with experiment, simply because the exact nature of the pinning centre is not known. The constant V_0 can be determined experimentally in various ways (eg., from low frequency “wall rocking” absorption measurements, or, less reliably, from a determination of the wall escape characteristics at higher T).

(b) For an insulating magnet, the principal contribution to wall dissipation at temperatures above the magnon gap Δ will come from multi-magnon emission by the wall⁵. However if $kT \ll \Delta$, the main magnon contribution to the dissipation will come from processes involving 2 bulk magnons and one wall, or “Winter”, magnon; this 3-magnon process gives an Ohmic contribution to the wall dissipation coefficient η , going like $\eta_3 \sim (kT/\Delta) \exp(-\Delta/kT)$. Higher magnon processes give contributions $\eta_m \sim (kT/\Delta)^{m-2} \exp(-\Delta/kT)$, and are thus subdominant. 2-magnon processes give a superOhmic contribution to the wall dissipation which is negligible compared to the Ohmic contribution at low energy or low wall velocity.

(c) When $kT \ll \Delta$, so that the magnons have negligible effects on the wall dynamics, an analysis has been given of 2 other small contributions to dissipation³: a coupling between the wall and Winter magnons, mediated by defects; and also a quite negligible coupling to photons. The influence of the defect-mediated coupling has recently been re-examined by Leduc and Stamp⁵⁶, with the conclusion that it can usually be neglected in practically relevant calculations.

(d) For a conducting magnetic system, a thorough analysis by Tatara and Fukuyama⁵⁷ showed that both the charge fluctuation (eddy current) and spin fluctuation contributions to the wall dissipation will be negligible unless the wall thickness is not much larger than the lattice separation between magnetic ions (even for SmCo₅, where $\lambda = 12\text{\AA}$, the electronic contribution gave a correction $< 1\%$ to the tunneling exponent).

(e) The phonon contribution to the dissipation of wall motion was analysed^{3,5} using the method of Wada and Schrieffer⁵⁸ to give a small T^3 contribution to the wall diffusion constant. This analysis was incomplete, since it did not include all one-phonon contributions to the dissipation; moreover, it did not include higher non-linear couplings, such as 2-phonon couplings. Since the 1-phonon coupling is superOhmic, experience with magnon couplings suggests one should go to higher order to look for Ohmic contributions to the wall dissipation. This is one of the main tasks of the present paper.

(f) One can also consider the possibility of “chirality tunneling” of the domain wall chirality^{59,60}, or even the coherent Bloch dynamics of walls in a periodic potential⁶¹. Until now no attempt has been made to see whether these possibilities would survive the coupling to the environment. This issue is also addressed herein; we find that they do not survive.

Amongst the various experimental searches for macroscopic domain wall tunneling, perhaps the most dramatic results are those of Giordano et. al.⁶⁻⁹. These results are in fairly good agreement with the theory, except that the experimental result for the quantum/classical crossover temperature (between tunneling and activated escape) is over an order of magnitude higher than the theoretical prediction⁵.

In this paper we will show that yet another modification of our understanding of the low- T dynamics of domain walls (and other magnetic solitons) is necessary. This is because of the inevitable coupling of the wall to the background nuclear spins, via hyperfine interactions. We shall see that the longitudinal hyperfine coupling energy $\sum_k \omega_k s_k^z I_k^z$, summed over all nuclear spins \mathbf{I}_k and electronic spins \mathbf{s}_k in the system, can be very large. The transverse hyperfine coupling $\sum_k \omega_k (s_k^+ I_k^- + s_k^- I_k^+)$ causes irreversible transitions in the nuclear spin bath every time the nanomagnetic system changes its state. This changes the energetics of the tunneling, and also causes “topological decoherence” and dissipation. These names are imported from the study of environmental “spin bath” effects on nanomagnetic tunneling^{43,46}, where similar physics applies.

We will not try here to give a complete analysis of nuclear spins effects on domain wall dynamics - this would be a very lengthy task. We concentrate instead on the static longitudinal hyperfine coupling. The main conclusion,

developed in detail below, is that domain wall tunneling is rendered much more complex by the coupling to nuclear spins and to phonons. The longitudinal hyperfine field is random in space, and fluctuates in time at a rate governed principally by T_2 relaxation. It can be very strong, and typically pins the domain wall. Tunneling can occur when temporal fluctuations in this potential open up “energy windows” for brief periods of time. The phonons also allow inelastic tunneling processes. Analysis of the various couplings to phonons shows that there are 3 important ones: a linear coupling to the domain wall velocity, a bilinear Ohmic coupling to the wall position, and an important linear Ohmic coupling to the wall chirality, which strongly suppresses any chirality tunneling, even in the absence of nuclear spins. As might have been expected, Bloch coherence is so fragile that it is destroyed by almost anything, and we believe it to be practically unobservable.

The plan of this paper is as follows. In the next section we discuss the various domain walls we will be dealing with in various geometries, including magnetic wires, magnetic films, and bulk 3-dimensional magnets. Essential results for the wall dynamics and tunneling in the absence of environmental effects are given, as well as relevant experimental numbers.

In section III we derive the effective low-energy interactions which couple a domain wall to both phonons and nuclear spins. The wall is coupled simultaneously to an “oscillator bath” of phonons, and a “spin bath” of nuclear spins, and a number of general results for such baths are recalled.

In section IV an extensive analysis is given of phonon effects on domain wall dynamics, for walls in 1, 2, and 3 dimensions, in isotopically purified magnets (no nuclear spins). The effective action for the wall is derived, with the phonons integrated out. These calculations are interesting theoretically, because of the novelty of some of the couplings. The dominant couplings to the wall velocity, the wall position, and the wall chirality are treated separately.

In section V the problem of wall tunneling is analysed. We first consider the “displacement tunneling” of walls in isotopically purified magnets, where it is controlled by phonons. We then include the nuclear spins, and show that tunneling is then strongly influenced by the dynamic hyperfine potential acting on the wall. For displacement tunneling this changes the theoretical predictions for the tunneling (in particular the crossover temperature and the tunneling rate). As a corollary to these calculations we analyse the suppression of both chirality tunneling and of Bloch coherence.

In the final section we make a few remarks on the relation to experiments on wall tunneling (particularly those of Giordano et al.).

II. DOMAIN WALLS AND THEIR ENERGETICS

In this section, we introduce the different kinds of domain wall we wish to study. Discussion of the couplings to the environment is reserved to later sections. We work exclusively with ferromagnetic systems, at low T , and we assume that the domain wall thickness λ is sufficiently greater than the lattice separation a_0 between spins so that a continuum approximation for the magnetisation is valid. We will be discussing domain walls in non-trivial geometries, including films and wires, as well as 3-dimensional systems.

In all cases, we assume that the magnetisation at position \mathbf{r} in the crystal is defined as $\mathbf{M}(\mathbf{r}) = g\mu_B \sum_j \mathbf{s}_j \delta(\mathbf{r} - \mathbf{R}_j)$, where μ_B is the Bohr magneton $\mu_B = e\hbar/2m_e c$, g is the Landé factor, and \mathbf{R}_j is the position of the j^{th} lattice site, with associated electronic spin \mathbf{s}_j .

There is no easy way to deal with the magnetic structure in bulk materials and in thin films and wires in a unified manner, as the direction of the magnetisation within the walls is quite different in these two cases. Instead of considering different values for the magnetisation in the (x, y, z) directions, we define in each case (bulk and thin films) a new frame of reference (x_1, x_2, x_3) such that the easy axis is along the x_1 direction, with the wall characterised by its position along the x_3 axis. The magnetisation is written as $\mathbf{M} = M_0 \hat{\mathbf{m}}$ with the unit vector $\hat{\mathbf{m}} = (m_x, m_y, m_z) = (\cos \phi \sin \theta, \sin \phi \sin \theta, \cos \theta)$ so that $(\nabla \mathbf{m})^2 = (\nabla \theta)^2 + \sin^2 \theta (\nabla \phi)^2$. We will assume that the magnitude M_0 is constant, since all phenomena considered occur at temperatures far below the Curie temperature. We thus use $M_0 = s\gamma_g \hbar/a_0^3$ where $\gamma_g = g\mu_B/\hbar$ is the gyromagnetic factor, a_0 is the lattice spacing of the crystal and s is the value of the electronic spin. We will assume a standard biaxial (easy axis/easy plane) Hamiltonian, given in continuum approximation by⁶²

$$\mathcal{H} = \frac{1}{2} \int d\mathbf{r} [J(\nabla \mathbf{M})^2 - K_{\parallel}(M_1)^2 + K_{\perp}(M_3)^2 - \frac{\mu_0}{2}(\mathbf{H}_{dm} + \mathbf{H}_e) \cdot \mathbf{M}] \quad (2.1)$$

where $(\nabla \mathbf{M})^2 \equiv (\nabla_i M_j)^2$. The easy axis is represented by the component M_1 of the magnetisation, and the easy plane is perpendicular to M_3 . K_{\parallel} and K_{\perp} are the anisotropy constants, \mathbf{H}_e is an external magnetic field and \mathbf{H}_{dm} is the demagnetising field⁶³, the internal field coming from all the magnetic moments.

The action of a the magnetisation also contains a term with no classical analogue, the Berry phase factor⁶⁴, or Wess-Zumino term⁶⁵, given by

$$S_{WZ} = i \int_0^{1/T} \int d\mathbf{r} \dot{\phi}(\mathbf{r}, t) (1 - \cos \theta(\mathbf{r}, t)) \quad (2.2)$$

so that the total action is $S = S_{WZ} + \int d\tau \mathcal{H}$. The Wess-Zumino term is purely imaginary. It essentially corresponds to the total solid angle traced by the spin configuration for a given trajectory; its derivation using path-integral or coherent spin state descriptions of the system is now very well known, following the 1983 work of Haldane⁶⁶.

1. Bloch Wall in Bulk Materials

For our study of the tunneling of a Bloch wall, we take the Hamiltonian

$$\begin{aligned} \mathcal{H} &= \int d\mathbf{r} [J(\nabla \mathbf{m})^2 - K_{\parallel} m_z^2 + K_{\perp} m_x^2] \\ &= \int d\mathbf{r} [J((\nabla \theta)^2 + \sin^2 \theta (\nabla \phi)^2) - K_{\parallel} \cos^2 \theta + K_{\perp} \cos^2 \phi \sin^2 \theta] \end{aligned} \quad (2.3)$$

representing a ferromagnet with easy z axis and easy $z - y$ plane. In 3-dimensions, J is measured in J/m, and the anisotropy constants in J/m³.

The domain wall corresponding to this Hamiltonian is perpendicular to the x axis, with the magnetisation rotating in the $z - y$ plane. The wall centre is located at a position Q along the x axis. The new frame of reference is thus $(x_1, x_2, x_3) = (z, y, x)$. This is represented in Fig.(1).

The components of the magnetisation are given by⁶²:

$$\begin{aligned} \hat{m}_1^B &= C \tanh \left(\frac{x_3 - Q(t)}{\lambda_B} \right) \\ \hat{m}_2^B &= \chi \left(1 - \frac{\dot{Q}^2(t)}{8c_0^2} \right) \text{sech} \left(\frac{x_3 - Q(t)}{\lambda_B} \right) \\ \hat{m}_3^B &= C \frac{\dot{Q}(t)}{2c_0} \text{sech} \left(\frac{x_3 - Q(t)}{\lambda_B} \right) \end{aligned} \quad (2.4)$$

where the thickness of the wall $\lambda_B = (J/K_{\parallel})^{1/2}$ represents the usual compromise between exchange and anisotropy. The surface energy of this type of wall is $\sigma_0 = 4(JK_{\parallel})^{1/2}$. $C = \pm 1$ is the “topological charge” of the wall and $\chi = \pm 1$ is the “chirality”. The topological charge corresponds to the direction along which the wall moves under the application of an external magnetic field in direction parallel to the easy axis, while the chirality refers to the sense of the rotation of the magnetisation inside the wall. The internal configuration of the wall is such as to simultaneously minimize the anisotropy energy (coming from both K_{\parallel} and K_{\perp}), and the exchange energy. The anisotropy K_{\perp} can originate from the material itself but also from the configuration of the magnetisation, through the demagnetisation energy⁶², ie., $K_{\perp} = K_{\perp,i} + \mu_0 M_0^2/2$ where $K_{\perp,i}$ is the anisotropy intrinsic to the material. A static Bloch wall only rotates in the easy plane. However, as soon as it moves it creates a demagnetising field which causes the spins to precess and the appearance of a component of the magnetisation out of the plane, directly proportional to the wall velocity^{62,67}. This picture is valid provided that $\dot{Q}(\tau) \ll c_0$, the Walker critical velocity, where⁶²

$$c_0 = \frac{2\gamma_g}{M_0} (JK_x)^{1/2} \left[\left[1 + \frac{K_{\perp}}{K_x} \right]^{1/2} - 1 \right] \quad (2.5)$$

where typically $c_0 \sim 10^2$ m/s. The precession of the spins also causes the appearance of an inertial term, the Döring mass, given by the ratio of the wall energy with the limiting velocity⁶²:

$$M_w = \frac{S_w M_0^2}{\gamma_g^2 (JK_{\parallel})^{1/2}} \left[\frac{1}{(1 + K_{\perp}/K_{\parallel})^{1/2} - 1} \right]^2 \quad (2.6)$$

where S_w is the surface of the wall. We assume $K_{\perp} \sim \mu_0 M_0^2/2 \gg K_{\parallel}$, and in this limit, $c_0 = \mu_0 \gamma_g \lambda M_0/2$ and the Döring mass reduces to $M_w = 2S_w/\mu_0 \gamma_g^2 \lambda$.

All of the above formulae for the Bloch wall are well known, and should be treated as phenomenological; they are given in terms of microscopic parameters, but should not be treated as the result of a microscopic derivation. In fact such a derivation would certainly give somewhat different results in the long-wavelength limit appropriate to the macroscopic dynamics of the wall, since integrating out the short wavelength fluctuations in $\mathbf{M}(\mathbf{r}, t)$ will renormalise all parameters. We do not bother to do this for 2 reasons, viz.,

(a) It is obvious that the renormalising influence of the high-frequency fluctuations will be strongly suppressed by the long-range demagnetisation field

(b) The only important parameter in any experimental tests of the theory will be the Doring mass, and this will have to be measured anyway (by, eg., looking at the fluctuation frequency of the wall in a pinning potential); the measured mass will of course then already incorporate the renormalisations.

Because of (a) we expect that the expressions in (2.5) and (2.6) to be fairly accurate anyway, and we will use them when necessary.

If defects are present in the sample, they can pin the wall. We will assume that the radius R_d corresponding to the defect volume is much smaller than λ_B , the domain wall width. The wall is then pinned by a potential of form⁵

$$V(Q) = -V_0 \text{sech}^2(Q/\lambda_B) \quad (2.7)$$

with V_0 proportional to the volume of the defect⁵. We further assume that there is a very small concentration of defects, so there is only 1 important pinning centre for the wall. This would correspond to an ideal experimental situation. We also assume that the wall is flat and that it remains flat during the tunneling process. This approximation is justified by the energy associated with the curvature of the wall, to which there are two contributions. The first is the surface energy σ_0 of the wall. A curved wall has a larger surface, and thus a larger energy. Second, and much more important, a curvature in the $x_1 - x_3$ plane creates strong long-range demagnetisation fields, which rapidly increase the wall energy. A complete treatment of these effects is quite complicated⁶², but for small pinning energies, the radius of curvature of the wall is much larger than λ , and it is easily shown that weak curvature has very little effect on wall tunneling^{3,68}. To consider the effect of dissipation, we can thus use a flat wall.

The application of an external magnetic field \mathbf{H}_e in the direction of the easy axis couples to the magnetisation to give a potential term linear in Q . Including the inertial mass, we then write a “bare” Hamiltonian (ie., neglecting the environment) for the wall⁵

$$H_w = \frac{1}{2} M_w \dot{Q}^2 - V(Q) - 2S_w \mu_0 M_0 H_e Q \quad (2.8)$$

where we put the chirality $C = 1$ for brevity.

The tunneling rate of the wall can now be evaluated by standard instanton techniques. For a field sufficiently close to the coercive field, the “pinning potential plus field potential” reduces to a quadratic plus cubic potential, whose barrier height is controlled by $\epsilon = 1 - H_e/H_c$, H_c being the coercive field, given as

$$\mu_0 H_c = \frac{2}{3\sqrt{3}} \frac{V_0}{\lambda S_w M_0} \quad (2.9)$$

while the energy barrier is

$$\tilde{V}(\epsilon) \sim (\hbar \gamma_g \mu_0 H_c) N_0 \epsilon^{3/2} \quad (2.10)$$

where N_0 is the number of spins in the wall. The exact value of the coercive field is of course very difficult to obtain theoretically and should ideally be obtained by a characterisation of the system in the thermal phase.

The tunneling rate Γ_0 in a cubic plus quadratic potential is well known^{3,5,13}; we simply recall here the results for the tunneling of the wall in the absence of dissipation:

$$\Gamma_0 = \left[\frac{30}{\pi} \frac{B(\epsilon)}{\hbar} \right]^{1/2} \Omega_0 e^{-B_0(\epsilon)/\hbar} \quad (2.11)$$

with $B_0(\epsilon)$ the usual WKB tunneling exponent;

$$\frac{1}{\hbar} B_0(\epsilon) = \frac{8}{15} M_w \Omega_0 Q_0^2 \quad (2.12)$$

Ω_0 the oscillation frequency of the wall in the potential;

$$\Omega_0^2 = \frac{3\sqrt{3}}{4}(\mu_0\gamma_g)^2(M_0H_c)\epsilon^{1/2}, \quad (2.13)$$

Q_0 is the escape point;

$$Q_0 = \frac{\sqrt{3}}{2}\lambda\epsilon^{1/2} \quad (2.14)$$

and λ is again the width of the wall. In terms of the microscopic parameters, $B_0(\epsilon)$ can be rewritten as

$$\frac{1}{\hbar}B_0(\epsilon) = \frac{54}{5}\frac{S_w\lambda}{\gamma_g\hbar}(M_0H_c)^{1/2}\epsilon^{5/4} \sim N_0\left(\frac{H_c}{M_0}\right)^{1/2}\epsilon^{5/4} \quad (2.15)$$

where the second form comes from using the number of spins in the wall, $N_0 = \lambda S_w/a^3$.

Although these results were originally derived for the particular case of a short-ranged defect pinning potential, they obviously have more general applicability; as emphasized previously^{3,5}, for small ϵ almost any pinning potential acting on the wall via the dipolar field or the wall surface energy will have the cubic-quadratic form near the coercive field, since its range will be $\sim \lambda$. However we shall see later in this paper that the same is *not* true of the longitudinal hyperfine field, coming from the nuclear spins, which fluctuates over much shorter length scales.

Let us at this point introduce 2 examples to which we will return at various points in this paper. We consider two particular systems, Yttrium Iron Garnet (YIG) and nickel. YIG is an insulator with a bcc cubic structure, a saturation magnetisation $\mu_0M_0 = 0.24$ T and with exchange and anisotropy energies $J = 1 \times 10^{-11}$ J/m and $K_{\parallel} = 580$ J/m³. The width of the domain wall is $\lambda = 860$ Å, with a mass per unit area 2×10^{-9} kg/m². Nickel is a conductor, again with a cubic structure. The saturation magnetisation $\mu_0M_0 = 0.6$ T, with exchange and anisotropy $J = 3 \times 10^{-11}$ J/m and $K_{\parallel} = 4500$ J/m³, giving a domain width $\lambda = 500$ Å and a mass 6×10^{-10} kg/m². As an example, we give the tunneling rate of a wall containing $N_0 = 10^6$ spins in nickel. Assuming $\epsilon = 10^{-3}$ and $H_c/M_0 = 0.01$, we get $B_0/\hbar \sim 20$, and a frequency $\Omega_0 \sim 6 \times 10^9$ sec⁻¹ so that $\Gamma \sim 200$ sec⁻¹.

The crossover temperature T_0 between thermally activated relaxation and quantum tunneling is roughly $k_B T_0 \sim \Omega_0/2\pi$. For many potentials (including the quadratic/cubic potential) there is a fast crossover between the two modes of relaxation (there are however systems, such as Mn₁₂Ac, where tunneling apparently takes place at intermediary levels, over a wide temperature range). For the Ni wall described above, $T_0 \sim 0.02$ K; a crossover temperature $T_0 \sim 0.1$ K would require the product $\mu_0H_c\epsilon^{1/4} \sim 0.6$ T, i.e., a coercive field similar to the magnetisation density.

2. Néel Walls in Thin Films

Bloch walls occur predominantly in bulk materials, and so are difficult to observe individually. Furthermore, they are fairly big, making the observation of tunneling difficult. If one tries to reduce the size of the sample to a wire or a platelet, then the Bloch wall becomes unstable and the magnetisation profile becomes quite complicated, most of the time being two-dimensional. One alternative is to go to thin films, of width $\delta \ll \lambda$, and with an anisotropy axis in the plane of the film. In this case, the strong demagnetisation field forces the rotation of the magnetisation between two domains to also take place in the plane of the film, in a head-on fashion. This is the model of the Néel wall^{67,69}. Its energy characteristics (ie., the Walker limiting velocity and the Doring mass), as well as the magnetisation profile are similar to that of a Bloch wall. We consider a film of length $L \gg \lambda$, width $\delta \ll \lambda$ in the $x_1 - x_3$ plane and with easy axis in the x_1 direction. The frame of reference of the wall is related to the Cartesian frame as $(x_1, x_2, x_3) = (y, z, x)$. This is shown in Fig. (2).

The continuum Hamiltonian is

$$\mathcal{H} = \int d\mathbf{r} [J(\nabla\mathbf{m})^2 - K_{\parallel}(\sin^2\theta \sin^2\phi - 1) + K_{\perp} \cos^2\theta] \quad (2.16)$$

The profile of the magnetisation is thus

$$\begin{aligned} \hat{m}_1^N &= C \tanh\left(\frac{x_3 - Q(t)}{\lambda}\right) \\ \hat{m}_3^N &= \chi \left(1 - \frac{\dot{Q}^2(t)}{8c_0^2}\right) \text{sech}\left(\frac{x_3 - Q(t)}{\lambda}\right) \\ \hat{m}_2^N &= C \frac{\dot{Q}(t)}{2c_0} \text{sech}\left(\frac{x_3 - Q(t)}{\lambda}\right) \end{aligned} \quad (2.17)$$

It is useful to ask what experimental set-up could test the theory of wall tunneling in this films. Stamp⁴⁴ discussed tunneling of a wall from a defect induced on the surface of the film (the ends of the wall being held fixed by artificially constructed “gate” defects - this avoids the problem of edges effects in the film).

3. Bloch and Néel Walls in Wires

The experiments of Giordano et. al.⁶⁻⁹ suggest that theoretical investigations of domain wall tunneling in wires, with diameter $d < \lambda$, might be very useful. It should immediately be emphasised that the question of the actual configuration of the magnetisation in such a wire is by no means simple, and suggestions that the magnetisation profile may be simply modelled as either a Bloch or Néel wall have been severely criticised by Aharoni⁷⁰. This point will arise again later in the present paper, when we come to consider the experiments of Giordano et. al. These experiments were analysed by the authors using the “displacement tunneling” model of wall tunneling^{3,5} just discussed; the influence of both phonons and magnons on the tunneling was ignored, in conformity with the results derived by Stamp.

Some rather more exotic tunneling processes have also been suggested for the cases where a simple Bloch or Néel wall configuration does occur in wires; these were given the names “chirality tunneling” and “Bloch coherence”. These possibilities were raised by Braun and Loss^{59,61} and by Takagi and Tataro⁶⁰. Since we will argue later in this paper that chirality tunneling and Bloch coherence are highly unlikely no matter what the wall looks like, the exact nature of the magnetisation profile is probably not important in what follows (on the other hand, it clearly *is* important in the analysis of Giordano’s experiments).

We consider first the possibility of chirality tunneling. For a Bloch wall, chirality tunneling corresponds to a tunneling of the sense of rotation of the wall (from clockwise to anti-clockwise, or vice-versa). The dynamical variable is $\phi(t)$, with tunneling being from $\phi = \pm\pi/2$ to $\phi = \mp\pi/2$, with θ constant, corresponding to the domain wall magnetisation rotating out of the easy plane. The tunneling splitting is very small - thus, for a wall in Ni wire, the tunneling splitting Δ_χ was estimated to be 0.1 MHz (ie., $5\mu\text{K}$, with a crossover to tunneling below $T_0 \sim 0.3\text{ mK}$).

For a Néel wall the situation is similar, except that the energy barrier is smaller, and so Δ_χ has been estimated to be as high as 80 mK. In both these cases the walls are assumed to be extremely small, containing perhaps 10^4 spins at most.

Braun and Loss also considered band or “Bloch” coherent motion of a 1-dimensional Néel wall (which they actually refer to as a Bloch wall). In the case of a Néel wall tunneling, the Berry phase of the wall enters in an important way; walls with integer phase have a the usual Brillouin zone, but walls with 1/2-integer phase have a halved Brillouin zone and the Bloch band is split into two bands, with opposite chirality. If one ignores all possible sources of decoherence from the environment, then a very small (10^4 spins) wall in YIG wire was estimated to have a Bloch bandwidth of $\Delta_d \sim 80\text{ mK}$. It was claimed that this motion should be observable when $T < T_c \sim 80\text{ mK}$.

III. COUPLING TO PHONONS AND NUCLEAR SPINS

As noted in section I, all quantum processes are strongly influenced by the coupling to the environment. Thus the formulae given in section II are a rough guide only; to properly determine the tunneling rate (or whether tunneling occurs at all) one must first include dissipative effects. This is of course even more true of any inelastic quantum diffusive dynamics, which only exists because of the coupling to the environment.

We now introduce the 2 different environments that will be studied. We begin with a few general remarks and useful formulae for oscillator baths and spin baths. We then go on to derive the various couplings between a domain wall and phonons. This is done for both 1-phonon and 2-phonon couplings. Finally, we derive the coupling between a domain wall and the nuclear spin bath, and show how this yields a slowly fluctuating spatially random potential acting on the wall.

A. Oscillator Bath and Spin Bath Environments

As already remarked in section I, we will be ignoring the effects of magnons, photons and electrons in what follows; in all cases this is because their dissipative effects are weak. We are nevertheless left with 2 important environmental couplings. Before giving a detailed treatment of these, we make some general remarks and recall some general formulae that will be relevant in the later technical discussions.

The phonon bath is representative of the oscillator bath model discussed by Feynman and Vernon⁷¹, and Caldeira and Leggett¹³. A subtlety that will arise here is that the individual oscillators do not necessarily represent individual

phonons: they can also represent pairs of phonons (an analogous situation was encountered in the discussion of magnon coupling to domain walls, where the oscillators represented triplets of magnons^{5,3}).

The nuclear spins on the other hand, are a good example of a “spin bath”, in which each environmental mode behaves as a 2-level system (with associated 2-level Hilbert space). In general the spin bath can behave quite differently from any oscillator bath^{43–47}.

The interaction between the nuclear spins and the phonons is utterly negligible. Thus the 2 baths act separately on the domain wall. Their effects are quite different and depend on the different nature of the 2 baths as follows:

(i) **Oscillator Baths** : This model assumes the environment can be described as a set of non-interacting harmonic oscillators, with each environmental mode weakly coupled to the system. For N delocalised environmental modes, the coupling between each oscillator and the system $\sim O(1/\sqrt{N})$ and the interaction between oscillators is $\sim O(1/N)$. The coupling between system and environment is *linear* in the bath coordinates. We emphasize that the connection between the oscillator modes and the modes that might appear in some microscopic model of the system can be non-trivial and non-linear. Provided such an oscillator bath exists, one may write a general Lagrangian now known as the Caldeira-Leggett Lagrangian¹³,

$$L_{CL} = \frac{M}{2}\dot{\mathbf{Q}}^2 + V(\mathbf{Q}) + \frac{1}{2} \sum_{\mathbf{k}} m_{\mathbf{k}} (\dot{\mathbf{x}}_{\mathbf{k}}^2 + \omega_{\mathbf{k}}^2 \mathbf{x}_{\mathbf{k}}^2) + \sum_{\mathbf{k}} [F_{\mathbf{k}}(\mathbf{Q}, \dot{\mathbf{Q}}) \mathbf{x}_{\mathbf{k}} + G_{\mathbf{k}}(\mathbf{Q}, \dot{\mathbf{Q}}) \dot{\mathbf{x}}_{\mathbf{k}}] + \Phi(\mathbf{Q}, \dot{\mathbf{Q}}) \quad (3.1)$$

where the environment is represented by the set $\{\mathbf{x}_{\mathbf{k}}\}$ and $\Phi(\mathbf{Q}, \dot{\mathbf{Q}})$ is a counterterm used when a phenomenological equation of motion is available; it simply cancels the shift in the potential introduced when the system is coupled to the oscillators.

An important simplification occurs if an expansion of $F_{\mathbf{k}}(\mathbf{Q}, \dot{\mathbf{Q}})$ and $G_{\mathbf{k}}(\mathbf{Q}, \dot{\mathbf{Q}})$ to first order in \mathbf{Q} and $\dot{\mathbf{Q}}$ is possible. A further set of transformations on the bath³² eliminates the coupling of the bath to $\dot{\mathbf{Q}}$, and then writing $F_{\mathbf{k}}(\mathbf{Q}) = C_{\mathbf{k}}\mathbf{Q}$, the Lagrangian is written as

$$L_{C-L} = L_0 + L_B + \frac{1}{2} \mathbf{Q} \sum_{\mathbf{k}} C_{\mathbf{k}} \mathbf{x}_{\mathbf{k}} - \frac{1}{2} \mathbf{Q}^2 \sum_{\mathbf{k}} \frac{C_{\mathbf{k}}^2}{m_{\mathbf{k}} \omega_{\mathbf{k}}^2} \quad (3.2)$$

where L_0 is the system Lagrangian and L_B the oscillator bath Lagrangian. The reduced density matrix of the system then defines the effective action^{13,71} $S_{eff} = S_0 + \Delta S_{eff}$, where S_0 is the system action and¹³

$$\Delta S_{eff} = \frac{1}{2} \int_0^{1/T} d\tau \int_0^{1/T} d\tau' \alpha(\tau - \tau') (\mathbf{Q}(\tau) - \mathbf{Q}(\tau'))^2 \quad (3.3)$$

with the kernel

$$\alpha(\tau - \tau') = \frac{1}{2\pi} \int_0^\infty d\omega J(\omega) D(\omega, |\tau - \tau'|) \quad (3.4)$$

where the environmental mode propagator $D(\omega, \tau)$ and spectral function $J(\omega)$ are

$$D(\omega, \tau) = \text{cosech}(\omega/2T) \cosh(\omega(\frac{1}{2T} - |\tau - \tau'|)) \quad (3.5)$$

$$J(\omega) = \frac{\pi}{2} \sum_{\mathbf{k}} \frac{C_{\mathbf{k}}^2}{m_{\mathbf{k}} \omega_{\mathbf{k}}} \delta(\omega - \omega_{\mathbf{k}}) \quad (3.6)$$

Alternatively, one can write

$$\alpha(\tau - \tau') = \frac{1}{4\pi} T \sum_n \int_0^\infty d\omega \omega J(\omega) \frac{e^{i\omega_n(\tau - \tau')}}{\omega_n^2 + \omega^2} \quad (3.7)$$

where $\omega_n = 2\pi nT$ is the bosonic Matsubara frequency⁷².

It should be emphasised that these effective Lagrangians, and the functions $\alpha(\tau)$ and $J(\omega)$, refer to a Hilbert space for both system and environment that has already been truncated to low energies. High energy environmental modes, as well as higher energy states of the system itself, are incorporated into the Lagrangian in the form of renormalised

couplings. Consequently the high-energy form of $J(\omega)$ typically has some smooth cut-off (for example of the form $J(\omega) \sim \exp(-\omega/\omega_c)$). At low frequency, $J(\omega)$ often has power law form. Most dissipation is caused by any term in $J(\omega)$ of Ohmic linear form, ie., for $J(\omega) = \eta\omega$ where η is the classical friction coefficient. In the absence of Ohmic dissipation, there will always be superOhmic terms of the form $J(\omega) \sim \omega^s$, with $s > 1$. Occasionally, one may also have to worry about a sharp jump in $J(\omega)$ at some finite frequency, usually imposed by a gap in some set of environmental modes. However in this case (a) other modes will always give contributions to $J(\omega)$ for ω below the gap energy, and (b) higher-order couplings to the same gapped modes are typically ungapped. Thus, for example, in the case of magnons coupled to a Bloch wall⁵, even though the magnon spectrum is gapped, one finds that coupling to pair of magnons gives an ungapped superOhmic ($J(\omega) \sim \omega^4$) term, and coupling to triplets of magnons gives an ungapped Ohmic term. Note, however, that such non-linear couplings to multiplets of bosonic excitation are always temperature-dependent, ie., $J(\omega) \rightarrow J(\omega, T)$.

In a tunneling situation, the strength of the coupling to the environment is determined by the dimensionless parameter $\alpha_t = \eta/2M_w\Omega_0$ for Ohmic coupling¹³, and we can define $\beta_t = \tilde{\beta}\Omega_0/M_w$ in the case of superOhmic dissipation with $s = 3$, when the spectral function $J(\omega) = \tilde{\beta}\omega^3$.

In the presence of friction, the crossover temperature from quantum tunneling to thermally activated relaxation is decreased. The new crossover temperature can be estimated in the case where $J(\omega)$ is T-independent,^{73,74}

$$T_c = T_0[(1 + \alpha_t^2)^{1/2} - \alpha_t] \quad (3.8)$$

for Ohmic dissipation. For superOhmic dissipation, in the weak dissipation regime ($\beta_t \ll 1$), $T_c = T_0(1 - \beta_t/2)$, while for strong coupling $T_c = T_0/\beta_t^{1/3}$ (again for a T-independent $J(\omega)$).

(ii) **Spin Baths:** In a wide variety of cases the environmental modes each have a finite Hilbert space. In the simplest case where this Hilbert space is 2-dimensional, each environmental mode is equivalent to some 2-level system, or to a spin-1/2. Examples of this include nuclear spins, paramagnetic impurities, as well as a variety of more subtle 2-level systems existing in glasses or disordered solids, often associated with defects. One should also note the various attempts to model the behaviour of dissipative quantum systems in terms of a set of 2-level ‘‘Landau-Zener’’ degrees of freedom⁷⁵.

Just as for the oscillator bath environment in Eq. (3.1), one may write a general description of a system interacting with a spin bath. It is more convenient to use a Hamiltonian formulation of this; the most general Hamiltonian form is then

$$H_{SB} = H_0(\mathbf{P}, \mathbf{Q}) + H_B(\{\boldsymbol{\sigma}_k\}) + H_{int}(\mathbf{P}, \mathbf{Q}, \boldsymbol{\sigma}_k) \quad (3.9)$$

where \mathbf{P} is conjugate to the system coordinate \mathbf{Q} , H_0 describes the system, and the spin bath has an Hamiltonian

$$H_B(\{\boldsymbol{\sigma}_k\}) = \sum_k \mathbf{h}_k \cdot \boldsymbol{\sigma}_k + \frac{1}{2} \sum_k \sum_{k'} V_{kk'}^{\alpha\beta} \sigma_k^\alpha \sigma_{k'}^\beta \quad (3.10)$$

in which the $\boldsymbol{\sigma}_k$ are Pauli spin matrix dynamical variables (with $k = 1, 2, \dots, N$), and the \mathbf{h}_k ’s are ‘‘external fields’’ which may exist. The couplings $V_{kk'}^{\alpha\beta}$ between the spins are often assumed to be much weaker than the characteristic energy scales of the system (for nuclear spins they are the very weak internuclear dipolar interactions; $|V_{kk'}| \sim 10^{-5}$ K or less).

The interaction Hamiltonian has the form

$$H_{int}(\mathbf{P}, \mathbf{Q}, \boldsymbol{\sigma}_k) = \sum_k \left(F_k^z(\mathbf{P}, \mathbf{Q}) \sigma_k^z + \frac{1}{2} (F_k^+(\mathbf{P}, \mathbf{Q}) \sigma_k^- + F_k^-(\mathbf{P}, \mathbf{Q}) \sigma_k^+) \right) \quad (3.11)$$

containing both ‘‘diagonal’’ couplings $F_k^z(\mathbf{P}, \mathbf{Q})$ which polarise the environmental spins) and ‘‘non-diagonal’’ couplings $F_k^\pm(\mathbf{P}, \mathbf{Q})$ (which flips them).

Whereas in the case of oscillator baths, averaging over the oscillators is conveniently done using path integrals (to produce an ‘‘influence functional’’), the lack of a well-defined classical path for the 2-level system makes such an approach infeasible here. Moreover, we stress that the couplings $F_k^\alpha(\mathbf{Q})$ are in general not small. This is in sharp contrast to the oscillator bath model, where the couplings $F_k(\mathbf{Q}) \sim O(N^{-1/2})$; in the spin bath the couplings are independent of N (so that their effects become more and more serious as N increases). For hyperfine interactions, $F_k^\alpha(\mathbf{Q})$ can be as high as 10 GHz (~ 0.5 K), for Ho nuclei - thus one can not always assume that a perturbative treatment of the $F_k^\alpha(\mathbf{Q})$ is valid.

To understand the effect of the spin bath on the dynamics of \mathbf{Q} , we make the assumption that $F_k^z(\mathbf{P}, \mathbf{Q}) \rightarrow F_k^z(\mathbf{Q})$. This is true for all cases studied so far (including domain walls). In this case, we may distinguish 2 effects.

On the one hand, the diagonal coupling $U(\mathbf{Q}) = \sum_k F_k^z(\mathbf{Q})\sigma_k^z$ acts as a random potential in the coordinate \mathbf{Q} ; we shall see this in detail for the case of a single domain wall. It is useful to define a density of states $W(U)$ for the potential U . In an ensemble of potentials (or of different systems), and assuming a typical value ω_0 for $F_k^z(\mathbf{Q})$, $W(U)$ is Gaussian in shape, of form

$$W(U) \sim (2\pi E_0^2)^{-1/2} \exp[-U^2/2E_0^2] \quad (3.12)$$

where $E_0 \sim N^{1/2}\omega_0$ is the gaussian half-width. In general the potential will fluctuate in time, because of transverse spin relaxation, at a rate governed by the nuclear T_2^{-1} (we will ignore T_1 processes in this paper, assuming that T_1 is very long). Thus $U(\mathbf{Q})$ also varies in time, and fluctuates, for any particular \mathbf{Q} , throughout the domain of $W(U)$. If $U(\mathbf{Q})$ were static, it would simply block the quantum dynamics of the system, by removing the degeneracy between initial and final tunneling states (we call this effect “degeneracy blocking”). Its fluctuations in time mean that “resonance windows” are occasionally opened between such states. Notice that the effect of $U(\mathbf{Q})$ is entirely elastic - no dissipation is involved.

On the other hand the non-diagonal couplings $F_k^\pm(\mathbf{P}, \mathbf{Q})$ cause environmental spins to *flip* under the action of the system. Thus, whereas the main effect of $F_k^z(\mathbf{Q})$ is to completely alter the effective potential acting on the system, the main effect of the non-diagonal couplings is to cause transitions in the spin bath, leading to dissipation and/or decoherence. Unlike the oscillator bath, dissipation and decoherence are not necessarily linked in the spin bath - indeed it is possible in certain cases to have decoherence without dissipation. Because the main effect of transitions in the spin bath is the absorption of a random topological Berry phase by the bath (thereby randomising the quantum phase associated with motion in \mathbf{Q}), this decoherence is called “topological decoherence”.

In this paper we shall develop the theory for a domain wall coupled to nuclear spins, but we shall ignore the dissipative effects coming from nuclear transitions. While these are not necessarily small, the “degeneracy blocking” effects, coming from the diagonal coupling $F_k^z(\mathbf{Q})$ are often considerably larger, particularly for weak hyperfine potentials (such as in Ni or Fe materials). Their main effect is the generation of a random potential acting on the wall, whose effects must be understood before dissipation is considered.

B. Phonon Couplings to the Wall

As noted above, it is not sufficient to consider only 1-phonon couplings to the wall; we must also consider non-linear 2-phonon couplings. These will be analysed using standard continuum elasticity theory for acoustic phonons coupled to the magnetisation; this rather intricate subject is reviewed by de Lacheisserie⁷⁸

The Euclidean Lagrangian of the acoustic phonons in a material of mass density ρ_v is

$$\mathcal{L}_p(\mathbf{x}, \tau) = \frac{1}{2}\rho_v \dot{u}_i^2 + \frac{1}{2}C_{ijkl}U_{ij}U_{kl} \quad (3.13)$$

where $u_i = \mathbf{r}_i - \mathbf{r}_i^0$ represents the phonon’s field, ie., the displacement of the atoms with respect to their equilibrium position, and $U_{kl} = (\partial_k u_l + \partial_l u_k)/2$ is the strain tensor. The potential energy of the field is given by the elastic tensor C_{ijkl} , with typical values $C \sim 10^{11}\text{J/m}^3$. The indices refer to the directions of the displacements, with the summation convention over repeated indices applied. We begin by considering an isotropic elastic energy, which is the simplest form

$$C_{ijkl} = \lambda_e \delta_{ij} \delta_{kl} + \mu_e (\delta_{ik} \delta_{jl} + \delta_{il} \delta_{jk}) \quad (3.14)$$

where μ_e and λ_e are the Lamé constants. The tensors that are going to be considered in this paper are all symmetric under the exchange of two indices forming a pair $\{ij\}$ and it is convenient to use the abbreviated notation

$$\begin{aligned} \{11\} &= 1 & \{22\} &= 2 & \{33\} &= 3 \\ \{23\} &= 4 & \{13\} &= 5 & \{12\} &= 6 \end{aligned} \quad (3.15)$$

We will thus represent any pair of indices by a letter $a = \{a_1 a_2\} = \{a_2 a_1\} = 1, \dots, 6$. This simplifies the notation tremendously.

We can also consider the phonons of a cubic structure. In this case, the non-zero elastic constants are $C_{11} = C_{22} = C_{33}$, $C_{12} = C_{13} = C_{23} = \dots$ and $C_{44} = C_{55} = C_{66}$. It reduces to the isotropic case if $C_{11} - C_{12} - 2C_{44} = 0$, in which case $C_{12} = \lambda_e$ and $C_{44} = 2\mu_e$.

It is observed experimentally that the shape of a fully magnetised ferromagnetic substance is different from the shape in the unmagnetised state. This phenomenon, called magnetostriction, can be related to the strain dependence of the anisotropy energy. There is thus an interaction between the direction of the magnetisation and the strain tensor of a solid. In many cases, this interaction is linear in the strain tensor. The simplest type of interaction that respects time-reversal symmetry is thus of the form $U_{ij}\hat{m}_k\hat{m}_l$, with i, j, k and l arbitrary directions. The interaction between phonons and the magnetisation is mediated by the first order magnetoelastic tensor, A_{ijkl} , as discussed in de Lacheisserie⁷⁸. It is also possible to consider an interaction that is quadratic in the strain and in the magnetisation, which is described by the second order magnetoelastic tensor R_{ijklmn} first introduced by Mason⁷⁹ and also discussed by de Lacheisserie⁷⁸. The general form of the interaction between the phonons and the domain wall is given by integrating over these local tensor couplings, throughout the sample, for a given wall profile, and then subtracting off the result that would have been obtained in the same integration in the absence of the wall. Thus, if the “vacuum” magnetisation profile is written as \mathbf{m}^0 , the general form of the interaction Lagrangian will be

$$L_{int} = - \int d^3\mathbf{r} A_{ijkl} U_{ij}(\mathbf{r}) (\hat{m}_k(\mathbf{r})\hat{m}_l(\mathbf{r}) - \hat{m}_k^0\hat{m}_l^0) + R_{ijklmn} U_{ij}(\mathbf{r}) U_{kl}(\mathbf{r}) (\hat{m}_m(\mathbf{r})\hat{m}_n(\mathbf{r}) - \hat{m}_m^0\hat{m}_n^0) \quad (3.16)$$

up to 2nd order in the phonon strain variables. The “vacuum” (no wall) term is just a constant (the integrated bulk magnetoelastic stress energy for the entire sample), which we subtract off in all our calculations.

From now on, we will use the definitions of the indices in Eq. (3.15) to discuss this Lagrangian. The first order tensor has been extensively studied in the context of magnetostriction. The second order tensor is encountered less frequently, but has been used in connection with the so-called “morphic effect”, i.e., the change in sound velocity as a function of the direction of the applied field⁷⁹. Both of these couplings come from an expansion of the exchange energy in terms of the displacement of the atoms. In our context, A and R then correspond to 1- and 2-phonon interaction terms respectively. Note that 2-phonon means that the interaction involves two phonons simultaneously, a process quite different from two 1-phonon processes^{27,80}.

For a crystal with orthorhombic symmetry, there are 12 non-zero matrix elements: $A_{11}, A_{22}, A_{33}, A_{12}, A_{21}, A_{13}, A_{31}, A_{23}, A_{32}, A_{66}, A_{55}$ and A_{44} . If the symmetry of the crystal is reduced to cubic, then $A_{11} = A_{22} = A_{33}$, $A_{44} = A_{55} = A_{66}$ and $A_{12} = A_{21} = A_{31} \dots$. The second order magnetoelastic tensor is obviously very complicated, but we will only use $R_{111} = R_{222} = R_{333}$ with all other R_{abc} equal to zero. This approximation is justified by the fact that these three components are generally of the same order of magnitude, while being at least two orders of magnitude larger than the other coefficients. Several measurements and calculations of these coefficients have been performed^{81,82}. In YIG, these are⁸³: $A_{ab} \sim 10^5 \text{ J/m}^3$, $R_{111} \sim 10^7 \text{ J/m}^3$, with the transverse sound velocity⁸⁴: $c_T \sim 3 \times 10^3 \text{ m/sec}$. In nickel⁸⁵: $A_{ab} \sim 10^8 \text{ J/m}^3$, $R_{111} \sim 10^{10} \text{ J/m}^3$, and $c_T \sim 10^3 \text{ m/sec}$.

We use the Fourier transform of the phonon field

$$\mathbf{u}(\mathbf{r}, \tau) = T \sum_n \sum_{\mathbf{q}} e^{-i\omega_n\tau + i\mathbf{q}\cdot\mathbf{r}} \mathbf{u}(\mathbf{q}, i\omega_n) \quad (3.17)$$

to write the action corresponding to the interaction Lagrangian, Eq. (3.16) as $S_I[\mathbf{u}, \hat{\mathbf{m}}] = S_I^{(i)}[\mathbf{u}, \hat{\mathbf{m}}] + S_I^{(ii)}[\mathbf{u}, \hat{\mathbf{m}}]$ with

$$S_I^{(i)}[\mathbf{u}, \hat{\mathbf{m}}] = \frac{i}{2} A_{ab} T \sum_n \sum_{\mathbf{q}} \int_0^{1/T} d\tau e^{i\mathbf{q}\cdot\mathbf{Q}(\tau)} e^{-i\omega_n\tau} \mathcal{M}_b(-\mathbf{q}) [q_{a1} u_{a2}(\mathbf{q}, i\omega_n) + q_{a2} u_{a1}(\mathbf{q}, i\omega_n)] \quad (3.18)$$

representing the action coming from 1-phonon processes and

$$S_I^{(ii)}[\mathbf{u}, \hat{\mathbf{m}}] = -\frac{1}{4} R_{abc} T^2 \sum_{nn'} \sum_{\mathbf{k}\mathbf{k}'} \int_0^{1/T} d\tau e^{i(\mathbf{k}+\mathbf{k}')\cdot\mathbf{Q}(\tau)} e^{-i(\omega_n+\omega_{n'})\tau} \mathcal{M}_c(-\mathbf{k}-\mathbf{k}') \times \\ [k_{a1} u_{a2}(\mathbf{k}, i\omega_n) + k_{a2} u_{a1}(\mathbf{k}, i\omega_n)] [k'_{b1} u_{b2}(\mathbf{k}', i\omega'_{n'}) + k'_{b2} u_{b1}(\mathbf{k}', i\omega'_{n'})] \quad (3.19)$$

corresponding to 2-phonon processes. $\mathbf{Q}(\tau)$ is the position of the wall and the summation convention over repeated magnetoelastic indices $a = \{a_1 a_2\}$ is in effect.

In these two expressions, the profile of the magnetisation is included in the magnetisation form factor \mathcal{M}_a defined as

$$\mathcal{M}_a(\mathbf{q}) = \int d^3\mathbf{r} e^{-i\mathbf{q}\cdot\mathbf{r}} (\hat{m}_{a1}(\mathbf{r})\hat{m}_{a2}(\mathbf{r}) - \hat{m}_{a1}^0(\mathbf{r})\hat{m}_{a2}^0(\mathbf{r})) \quad (3.20)$$

The magnetoelasticity of thin films differs considerably from what is observed in the bulk⁷⁸. The elastic properties and the symmetry of a film will in general be different than those in bulk, and the strain associated with the surface

will also play a major role. The magnetostriction constants in general are dependent on the thickness of the film and, furthermore, in many cases when discussing the simple magnetostriction, it is impossible to consider only the linear magnetostriction. It turns out that it is strain dependent and that the second order magnetoelastic constants play a major role^{78,86}. It is obvious that a proper discussion of the magnetoelastic dissipation requires a very detailed knowledge of the material being used. To keep the discussion general, we still use the Lagrangian Eq. (3.16) where now the phonons will be 2-dimensional, with a surface density ρ_s and the elastic and magnetoelastic constants have units of J/m². Similarly, in 1 dimension, we consider a linear density ρ_l and the constants have units of J/m. More detailed models could be devised if necessary.

Finally, a special comment must be made about the terms in the magnetisation profile appearing due to the finite velocity of the wall, ie., coming from the demagnetisation energy. They represent a coupling to the environment that is proportional to the velocity of the macroscopic coordinate. The standard way to deal with this coupling is to introduce a total time derivative term in the action and to perform a canonical transformation to a new set of oscillators (c.f. Leggett³²). In our case, it does not appear that this can be done easily since the coupling is not “strictly linear”, but is a complicated function of \mathbf{Q} . We will first build the effective action of the magnetisation including the velocity term. This will allow us to see in which cases exactly this coupling to the velocity is important. Once its physical relevance or irrelevance is established, it is easy to go back to the original Lagrangian and to deal with this term directly.

C. Nuclear Spin Coupling to the Wall

Nuclear hyperfine effects vary enormously between magnetic systems. The weakest is in Ni, where only 1% of the nuclei have spins, and the hyperfine coupling is only $\omega_0 = 28.35$ MHz (~ 1.4 mK). On the other hand, in the case of rare earths, ω_0 varies from 1 to 10 GHz (0.05 to 0.5 K). In this latter case the hyperfine coupling energy to a *single* nucleus may be comparable to the other energy scales in the problem !

To derive an effective interaction Hamiltonian, we consider our system of ferromagnetically ordered spins to coupled locally to N nuclear spins \mathbf{I}_k at positions \mathbf{r}_k ($k = 1, 2, 3, \dots, N$), which for a set of dilute nuclear spins (where only one isotope has a nuclear spin) will be random. The total Hamiltonian for the coupled system is then

$$H = H_m + \sum_{k=1}^N \omega_k \mathbf{s}_k \cdot \mathbf{I}_k + \frac{1}{2} \sum_k \sum_{k'} V_{kk'}^{\alpha\beta} I_k^\alpha I_{k'}^\beta \quad (3.21)$$

where H_m is the electronic Hamiltonian for the magnetisation (Eq. (2.1)), written in terms of the electronic spins \mathbf{s}_k at the sites where there happen to be nuclear spins, and ω_k is the hyperfine coupling at \mathbf{r}_k ; $V_{kk'}^{\alpha\beta}$ is the internuclear dipolar interaction, with strength $|V_{kk'}^{\alpha\beta}| \sim 1 - 100$ kHz ($0.05 - 0.5$ μ K). In terms of the continuum magnetisation $\mathbf{M}(\mathbf{r})$, we have

$$H = H_m + \sum_{k=1}^N \omega_k \int \frac{d^3r}{\gamma_g} \delta(\mathbf{r} - \mathbf{r}_k) [M_z(\mathbf{r}) I_k^z + (M_x(\mathbf{r}) I_k^x + M_y(\mathbf{r}) I_k^y)] + \frac{1}{2} \sum_k \sum_{k'} V_{kk'}^{\alpha\beta} I_k^\alpha I_{k'}^\beta \quad (3.22)$$

The resemblance between this form and the spin bath coupling form given above is evident - however, it is often more convenient to rewrite Eq. (3.22) by separating out the slowly-varying wall profile $\mathbf{M}_W(\mathbf{r})$ from the “fast” magnon fluctuations which ride on top of this. Thus we write

$$\mathbf{M}(\mathbf{r}) = \mathbf{M}_W(\mathbf{r}, Q) + \delta\mathbf{M}(\mathbf{r}) \quad (3.23)$$

where $\mathbf{M}_W(\mathbf{r}, Q)$ is the wall profile for a wall centered at Q (given in Eq. (2.4) for a Bloch wall and Eq. (2.17) for a Néel wall). We then introduce local axes (u, v, w) , with $\hat{\mathbf{x}}_w$ parallel to $\mathbf{M}_W(\mathbf{r}, Q)$, and $\hat{\mathbf{x}}_u, \hat{\mathbf{x}}_v$ perpendicular to it, and to each other (these axes were called x_1, x_2, x_3 in previous papers^{3,5}). Then we quantise the $\delta\mathbf{M}(\mathbf{r})$ in terms of local magnon operators $b(\mathbf{r})$ and $b^+(\mathbf{r})$, as usual:

$$\begin{aligned} \delta M_w(\mathbf{r}) &= -4\gamma_g b^+(\mathbf{r}) b(\mathbf{r}) \\ \delta M_+(\mathbf{r}) &= (4\gamma_g M_0)^{1/2} \left(1 - \frac{2\gamma_g}{M_0} b^+(\mathbf{r}) b(\mathbf{r}) \right)^{1/2} b(\mathbf{r}) \\ \delta M_-(\mathbf{r}) &= (4\gamma_g M_0)^{1/2} b^+(\mathbf{r}) \left(1 - \frac{2\gamma_g}{M_0} b^+(\mathbf{r}) b(\mathbf{r}) \right)^{1/2} \end{aligned} \quad (3.24)$$

where $\delta M_{\pm}(\mathbf{r}) = \delta M_u(\mathbf{r}) \pm \delta M_v(\mathbf{r})$. The interaction term in Eq. (3.22) is now written for a single domain wall by again subtracting off the “vacuum” magnetisation profile \mathbf{M}_0 obtaining in the absence of the wall, to get a sum of longitudinal and transverse couplings:

$$H_{int}(Q, \{\mathbf{I}_k\}) = {}^{\parallel}H_{int} + {}^{\perp}H_{int} \quad (3.25)$$

$${}^{\parallel}H_{int} = \sum_{k=1}^N \omega_k \int \frac{d^3r}{\gamma_g} \delta(\mathbf{r} - \mathbf{r}_k) ((M_W(\mathbf{r}, Q) I_k^w - \mathbf{M}_0 \cdot \mathbf{I}_k) + I_k^w \delta M_w(\mathbf{r})) \quad (3.26)$$

$${}^{\perp}H_{int} = \frac{1}{2} \sum_{k=1}^N \omega_k \int \frac{d^3r}{\gamma_g} \delta(\mathbf{r} - \mathbf{r}_k) (\delta M_+(\mathbf{r}) I_k^- + \delta M_-(\mathbf{r}) I_k^+) \quad (3.27)$$

To get an idea of the size and effect of each of these terms, let us choose as example a Bloch wall, supposing for simplicity that $\omega_k = \omega_0$ for each nuclear spins (in reality the $\{\omega_k\}$ will be spread out by the internuclear $V_{kk'}^{\alpha\beta}$, as well as by transfer hyperfine couplings to non-magnetic ions).

Supposing also that the Bloch wall is static, we have, from Eq. (2.4), for a wall centered at $x_3 = Q$, a static longitudinal interaction

$${}^{\parallel}H_{int}^{Bloch}(Q, \{\mathbf{I}_k\}) = \frac{\omega_0 M_0}{\gamma_g} \sum_{k=1}^N \int d^3r \delta(\mathbf{r} - \mathbf{r}_k) \left(\left(1 - C \tanh \left(\frac{x_3 - Q}{\lambda_B} \right) \right) + \delta m_w(\mathbf{r}) \right) I_k^w \quad (3.28)$$

and a transverse interaction

$$\begin{aligned} {}^{\perp}H_{int}^{Bloch}(Q, \{\mathbf{I}_k\}) &= \frac{\omega_0 M_0}{2\gamma_g} \sum_{k=1}^N \int d^3r \delta(\mathbf{r} - \mathbf{r}_k) \left(\chi \operatorname{sech} \left(\frac{x_3 - Q}{\lambda_B} \right) (I_k^+ + I_k^-) \right. \\ &\quad \left. + (\delta m_-(\mathbf{r}) I_k^+ + \delta m_+(\mathbf{r}) I_k^-) \right) \end{aligned} \quad (3.29)$$

where $\delta \mathbf{m} = \delta \mathbf{M}/M_0$.

We can extract from Eq. (3.28) and (3.29) the following 3 terms:

(i) Terms of the form $I_k^{\alpha} \delta \mathbf{m}_{\beta}$ couple nuclear spins to magnons; this interaction is considerably enhanced inside the wall where the magnons are gapless, and is known to be important in the discussion of the NMR relaxation rate inside the wall.

(ii) We also have a longitudinal $\tanh[(x_3 - Q)/\lambda_B]$ term in ${}^{\parallel}H_{int}$ which is diagonal in the local nuclear spin basis states (with axis of quantisation $\hat{\mathbf{x}}_w$ along $\mathbf{M}_W(\mathbf{r}, Q)$). This term gives us a random potential when summed over all spins, which we write as

$$U(Q) = \frac{\omega_0 M_0}{\gamma_g} \sum_{k=1}^N \int d^3r \delta(\mathbf{r} - \mathbf{r}_k) \left(1 - C \tanh \left(\frac{x_3 - Q}{\lambda_B} \right) \right) I_k^w \quad (3.30)$$

Suppose we use the “high-T” limit, where $kT \gg \omega_0$, so that the expectation value $\langle \mathbf{I}_k \rangle$ is zero in any direction. Since the nuclear spins are completely uncorrelated ($V_{kk'}^{\alpha\beta}$ is negligible), a volume containing N nuclear spins will have root mean square polarisation $\sim N^{1/2}$. It then immediately follows that for a system in which a fraction x of all the states are occupied by nuclear spins \mathbf{I}_k at sites k , the ensemble averaged correlation between $U(Q)$ for 2 different wall position is

$$\begin{aligned} \mathcal{C}_{UU}(Q_1 - Q_2) &= \langle (U(Q_1) - U(Q_2))^2 \rangle \sim \omega_0^2 s^2 I^2 \Delta N_{Q_1 - Q_2} \\ &\sim \left(\frac{\omega_0 M_0 I}{\gamma_g} \right)^2 a_0^3 x S_w (Q_1 - Q_2) \quad (T \gg \omega_0) \end{aligned} \quad (3.31)$$

where $s = |\mathbf{s}_k|$, $I = |\mathbf{I}_k|$, S_w is the area of the wall, and $\Delta N(Q_1 - Q_2) \sim (x S_w / a_0^3) (Q_1 - Q_2)$ is the mean number of nuclear spins in the volume swept out by the wall in going from Q_1 to Q_2 . Thus $U(Q)$ exhibits “random walk” behaviour over the sample⁸⁸, as represented on Fig. (3).

Eq. (3.31) is for the high- T limit. In the case of very low T , when $T \ll \omega_0$, the nuclear spins will tend to line up in the field due to the electronic moments. In the low- T limit, they will all be aligned according to the wall configuration, and Eq. (3.31) is replaced by

$$\mathcal{C}_{UU}(Q_1 - Q_2) \sim \left(\frac{\omega_0 M_0 I}{\gamma_g} \right)^2 a_0^6 x^2 S_w^2 (Q_1 - Q_2)^2 \quad (3.32)$$

Thus the wall is trapped in a potential which increases linearly (on average) in both directions away from the wall centre. In reality, both results (3.31) and (3.32) are only valid for times $\ll T_2$; for larger times the internuclear dipolar transitions cause random fluctuations of the hyperfine potential.

(iii) Finally, we have the $\text{sech}[(x_3 - Q)/\lambda_B]$ term in Eq. (3.29), acting only inside the wall; this simply tells us that in the chirally-rotated frame of $\mathbf{M}_W(\mathbf{r}, Q)$, the nuclear spins quantised along the “vacuum” \mathbf{M}_0 are no longer diagonal. Because of this term, a domain moving through a field of nuclear spins can flip some of them as it passes, thereby causing both topological decoherence and dissipation in general. From the solution of the “central spin” problem⁴³ one may estimate that the mean number λ_I of flipped spins caused by a single excursion between 2 points Q_1 and Q_2 (sweeping out ΔN nuclear spins) will be given by

$$\lambda_I \sim \frac{1}{2} \Delta N \left(\frac{\pi \omega_0}{2 \Omega_0} \right)^2 \quad (3.33)$$

where Ω_0 is the typical frequency involved in the motion from Q_1 to Q_2 (Ω_0 being the bounce frequency for tunneling motion), provided $\omega_0 \ll \Omega_0$.

To get a feeling for the numbers, consider the “high- T ” limit $k_B T \gg \omega_0$. Now imagine a wall of area $(300 \times 300) \text{\AA}^2$, which sweeps out a length $Q_1 - Q_2 \sim 300 \text{\AA}$, and a volume containing $\sim 10^6$ electronic spins (ie., $a_0 \sim 3 \text{\AA}$); suppose also that $S = |\mathbf{S}_k| = 1$ and $I = |\mathbf{I}_k| = 1/2$. We may imagine 2 extreme cases:

(a) Suppose ω_0 is very small, eg., let $\omega_0 = 1.4 \text{ mK}$, and let $x = 0.01$ (only 1% of nuclei have spins); these are values appropriate to Ni. Then the Gaussian mean change in $U(Q)$ for the wall will be $|\Delta U| \sim 0.3 \text{ K}$, in the high- T limit (ie., $T \gg 1.4 \text{ mK}$; all experiments up to now have been in this limit). If we assume that $\Omega_0 \sim 2 \times 10^{10} \text{ Hz}$ (typical of wall tunneling), then $\lambda_I \sim 0.025$, ie., in most cases no nuclei will be flipped at all.

(b) Suppose now $\omega_0 = 0.2 \text{ K}$, a value more typical of some rare earth magnets, and that $x = 1$. We then have, in the high- T limit (now for $T \gg 0.2 \text{ K}$), that $|\Delta U| \sim 400 \text{ K}$, and $\lambda_I \sim 10^5$ (each nucleus has a probability ~ 0.1 of being flipped) ! Even if we reduce the displacement in this case from 300\AA to only 3\AA (ie., the wall makes only a single lattice displacement), we still find $|\Delta U| \sim 40 \text{ K}$ and $\lambda_I \sim 10^3$.

Notice furthermore that the low- T limit $k_B T \ll \omega_0$, where all nuclear spins line up with the local magnetisation, is easily attainable for rare earth systems, in current experiments. In this case the effects are spectacular; for the present example, with $\omega_0 = 0.2 \text{ K}$, a displacement of 300\AA leads to an energy change $|\Delta U| \sim 20 \text{ eV}$!! Thus the wall is completely locked to the nuclear polarisation when $k_B T \ll 0.2 \text{ K}$.

Thus in the first case, of extremely weak coupling, we see that dynamic effects in the bath can be ignored - the sole function of the nuclear bath is to provide a weak random static potential. On the other hand in the case of rare-earth magnets, with very strong hyperfine coupling, the nuclear effects are quite enormous, and moreover it is crucial to take account of nuclear transitions in analysing the wall motion.

In this paper we will concentrate on the weak coupling case, because it is simpler and more relevant to the Ni wire experiments of Giordano et. al. We shall deal in section V with the residual effects of the internuclear coupling, which drives the slow (on the scale of Ω_0^{-1}) fluctuations in time of $U(Q)$.

IV. EFFECTIVE ACTION OF A DOMAIN WALL COUPLED TO PHONONS

In this section, we obtain the effective action of a domain wall interacting with the phonons through the magnetoelastic interaction⁷⁸; we completely ignore the nuclear spins in this section. We consider both 1-phonon and 2-phonon processes, as described in the last section, and we relate their effect to the phenomenological oscillator bath of Caldeira and Leggett¹³. As expected 1-phonon processes give rise to superOhmic dissipation with $J(\omega) \sim \omega^3$. We find however that the dominant contribution to the dissipation comes from the coupling between the *velocity* of the wall and the phonons.

The second order magnetoelastic tensor brings in 2-phonon mediated Ohmic dissipation, with a temperature dependent friction coefficient $\eta(T) \sim T^{3+d}$ (where d is the effective dimensionality of the phonons), just as with the quantum diffusion of a particle in an insulator⁸⁰. In this case however, the coupling to the velocity of the wall is unimportant. As part of our the discussion of 2-dimensional 2-phonon processes, we discuss the general case of the

dissipation of a Néel wall. This represents a straightforward extension of the analysis of a Bloch wall. The same is true for the dissipation in a wire, where the phonons are effectively 1-dimensional.

A. Effective Action of a Bloch Wall

We are interested in integrating out the phonons so as to obtain an effective action for the magnetisation. The effective action is defined as

$$\begin{aligned} e^{-S_{eff}[\hat{\mathbf{m}}]} &= e^{-S_0[\hat{\mathbf{m}}]} \frac{\int D[\mathbf{u}] e^{-S_0[\mathbf{u}] - S_I[\hat{\mathbf{m}}, \mathbf{u}]}{\int D[\mathbf{u}] e^{-S_0[\mathbf{u}]}} \\ &= e^{-S_0[\hat{\mathbf{m}}]} \langle e^{-S_I[\hat{\mathbf{m}}, \mathbf{u}]} \rangle \end{aligned} \quad (4.1)$$

where S_0 is the action of the phonons and S_I is the magnetoelastic interaction, as described in the Introduction. We recall that the interaction action $S_I = S_I^{(i)} + S_I^{(ii)}$, representing 1- and 2-phonon processes, is expressed as the sum of Eq. (3.18) and Eq. (3.19). The uniform magnetisation, in absence of a domain wall, is in the x_1 direction. The form factor of the magnetisation, appearing in the action S_I is thus

$$\mathcal{M}_a(\mathbf{q}) = \int d^3\mathbf{r} e^{-i\mathbf{q}\cdot\mathbf{r}} (\hat{m}_{a_1}(\mathbf{x}) \hat{m}_{a_2}(\mathbf{r}) - \delta_{a_1,1} \delta_{a_2,1}) = (2\pi)^2 \delta(q_1) \delta(q_2) \mathcal{M}_a(q_3) \quad (4.2)$$

This last form coming from the one-dimensional properties of a Bloch wall. The magnetisation depends only on the coordinates normal to the wall and this restricts the momentum in the plane of the wall to be zero. Using the description of a Bloch wall in term of the component of the magnetisation Eq. (2.4), it is easy to compute these different terms. Up to second order in the velocity of the wall, they are:

$$\mathcal{M}_1^B(q_3) = -\pi q_3 \lambda^2 \text{cosech}(\pi q_3 \lambda / 2) \quad (4.3)$$

$$\mathcal{M}_2^B(q_3, \tau) = \left(1 - \frac{\dot{Q}^2(\tau)}{4c_0^2} \right) \pi q_3 \lambda^2 \text{cosech}(\pi q_3 \lambda / 2) \quad (4.4)$$

$$\mathcal{M}_3^B(q_3, \tau) = \frac{\dot{Q}^2(\tau)}{4c_0^2} \pi q_3 \lambda^2 \text{cosech}(\pi q_3 \lambda / 2) \quad (4.5)$$

$$\mathcal{M}_4^B(q_3, \tau) = \frac{\dot{Q}(\tau)}{2c_0} \pi q_3 \lambda^2 \text{cosech}(\pi q_3 \lambda / 2) \quad (4.6)$$

$$\mathcal{M}_5^B(q_3, \tau) = -i \frac{\dot{Q}(\tau)}{2c_0} \pi q_3 \lambda^2 \text{sech}(\pi q_3 \lambda / 2) \quad (4.7)$$

$$\mathcal{M}_6^B(q_3, \tau) = -i \left(1 - \frac{\dot{Q}^2(\tau)}{8c_0^2} \right) \pi q_3 \lambda^2 \text{sech}(\pi q_3 \lambda / 2) \quad (4.8)$$

where $\lambda = (J/K_{\parallel})^{1/2}$ is the domain wall width and c_0 is the Walker velocity, defined in Eq. (2.5). There are essentially two types of coupling; those proportional to $\text{cosech}(\pi q_3 \lambda / 2)$, which go to the constant 2λ as $q_3 \rightarrow 0$, while those proportional to $\text{sech}(\pi q_3 \lambda / 2) \rightarrow 0$ as $q_3 \rightarrow 0$. This already indicates that dissipative terms involving \mathcal{M}_1 , \mathcal{M}_2 , \mathcal{M}_3 and \mathcal{M}_4 will be more important than those coming from \mathcal{M}_6 and \mathcal{M}_5 .

It should be noticed that there is a natural cutoff momentum $k_c = 2/(\pi\lambda)$ coming directly from the wall structure. This can be converted to a cutoff frequency $\omega_c = 2c_T/(\pi\lambda)$. For a wall of width $\lambda = 500\text{\AA}$, and with a transverse sound velocity $c_T \sim 10^4\text{ m/s}$, this gives a cutoff frequency $\omega_c = 10^{11}\text{ Hz}$. Walls with a very small width will have an even larger ω_c . This cutoff frequency is usually much larger than the bounce frequency Ω_0 , defined in Eq. (2.13), at which the bath must be cutoff from the truncation procedure. This makes it possible to use $\text{cosech}(\omega/\omega_c) \sim \omega_c/\omega$ and $\text{sech}(\omega/\omega_c) \sim 1$.

The exact form of the magnetisation profile is actually not too critical; we are mostly interested in the behaviour of these form factors at low- q . They are essentially an integral of the components of the non-uniform magnetisation out of the easy axis. The spatial variation of these terms is actually what defines the width of the wall, so it is quite clear that the relevant form factors for the dissipative dynamics of the wall behave as

$$\lim_{q \rightarrow 0} \mathcal{M}(q) \rightarrow \mathcal{B}_\lambda \lambda \quad (4.9)$$

where \mathcal{B}_λ is a coefficient of $O(1)$ depending on the precise profile of the magnetisation and λ is the length scale over which the magnetisation changes from one stable configuration to another. This should be accurate provided that the curvature of the wall is weak, of course.

The two-point function of the phonon field is decomposed as usual into a transverse and longitudinal part⁸⁷

$$\langle u_i(\mathbf{p}, i\omega_n) u_j(-\mathbf{p}, -i\omega_n) \rangle = (\delta_{ij} - \hat{p}_i \hat{p}_j) G^T(\mathbf{p}, i\omega_n) + \hat{p}_i \hat{p}_j G^L(\mathbf{p}, i\omega_n) \quad (4.10)$$

with

$$G^{T,L}(\mathbf{p}, i\omega_n) = \frac{1}{\rho_v} \frac{1}{c_{T,L}^2 p^2 + \omega_n^2} \quad (4.11)$$

where $c_T^2 = \mu_e / \rho_v$ and $c_L^2 = (\lambda_e + 2\mu_e) / \rho_v$ are the transverse and longitudinal sound velocities.

The effective action is found from a simple cumulant expansion. The first term, $\langle S_I \rangle$ is ignored: the 1-phonon term $\langle S_I^{1ph} \rangle$ is zero due to $\langle \mathbf{u} \rangle = 0$, and the 2-phonon term is independent of $Q(\tau)$, simply adding a contribution to the potential energy of the phonons (morphic effect). The ratio of the second-order magnetoelastic constants to the elastic energy is generally less than 1% and we can simply ignore this renormalisation in the sound velocity. The first dissipative contribution to the effective action is thus $\langle S_I^2 \rangle / 2 = \langle (S_I^{1ph})^2 \rangle / 2 + \langle (S_I^{2ph})^2 \rangle / 2$ which gives

$$\begin{aligned} \Delta S_{eff} = & \frac{1}{2} A_{ab} A_{cd} T \sum_n \sum_{\mathbf{q}} \int_0^{1/T} d\tau d\tau' e^{i\omega_n(\tau-\tau')} e^{iq_3 \cdot (Q(\tau) - Q(\tau'))} \mathcal{M}_b(-\mathbf{q}) \mathcal{M}_d(\mathbf{q}) \mathcal{G}_{ac}(\mathbf{q}, i\omega_n) \\ & + \frac{1}{2} R_{abc} R_{def} T^2 \sum_{\mathbf{k}\mathbf{k}'} \sum_{nn'} \int_0^{1/T} d\tau d\tau' e^{i(\omega_n + \omega_{n'}) (\tau - \tau')} e^{i(k_3 + k'_3) \cdot (Q(\tau) - Q(\tau'))} \mathcal{M}_c(-\mathbf{k} - \mathbf{k}') \\ & \times \mathcal{M}_f(\mathbf{k} + \mathbf{k}') [\mathcal{G}_{ad}(\mathbf{k}, i\omega_n) \mathcal{G}_{be}(\mathbf{k}', i\omega_{n'}) + \mathcal{G}_{ae}(\mathbf{k}, i\omega_n) \mathcal{G}_{bd}(\mathbf{k}', i\omega_{n'})] \end{aligned} \quad (4.12)$$

where $\mathcal{G}_{ab} \equiv \frac{1}{4} (k_{a_1} k_{b_1} G_{a_2 b_2}(\mathbf{k}, i\omega_n) + \text{Perm})$. The index $a \equiv (a_1, a_2)$ is the pair of the indices introduced in Eq. (3.15) and Perm indicates the permutations $a_1 \leftrightarrow a_2$ and $b_1 \leftrightarrow b_2$. A third term, of the form $\mathcal{G}_{ab} \mathcal{G}_{de}$, is generated in the effective action, but it does not couple to the position of the wall, simply corresponding to a further renormalisation of the sound velocity. Since it is not a dissipative term we do not include it in the effective action. It is now possible to examine the different contributions to this action.

B. 1-Phonon Contributions to Action

The 1-phonon part of the action is very simple. Summing over the frequency, and separating the action into a transverse and a longitudinal part, we obtain

$$\Delta S_{eff}^{1ph} = \Delta S_{eff}^{1ph T} + \Delta S_{eff}^{1ph L} \quad (4.13)$$

$$\begin{aligned} \Delta S_{eff}^{1ph, T} = & \frac{1}{c_T} \frac{S_w}{\rho_v} \int_0^\infty \frac{2dq_3}{2\pi} \int_0^{1/T} d\tau d\tau' \cos(q_3(Q(\tau) - Q(\tau'))) q_3 D(c_T q_3, |\tau - \tau'|) \times \\ & [A_{55}^2 \mathcal{M}_5(-q_3) \mathcal{M}_5(q_3) + A_{44}^2 \mathcal{M}_4(-q_3) \mathcal{M}_4(q_3)] \end{aligned} \quad (4.14)$$

$$\begin{aligned} \Delta S_{eff}^{1ph, L} = & \frac{1}{4c_T} \frac{S_w}{\rho_v} \int_0^\infty \frac{2dq_3}{2\pi} \int_0^{1/T} d\tau d\tau' \cos(q_3(Q(\tau) - Q(\tau'))) q_3 D(c_L q_3, |\tau - \tau'|) \\ & A_{3a} A_{3b} \mathcal{M}_a(-q_3) \mathcal{M}_b(q_3) \end{aligned} \quad (4.15)$$

where $D(\omega, \tau)$ is the boson propagator, defined in Eq. (3.5). This simple form of the effective action is obtained by taking advantage of the fact that for a Bloch wall $q_1 = q_2 = 0$. Next, inserting the expressions for the \mathcal{M}_a 's, we obtain terms that contain only the position of the wall, of the form $\cos \omega(Q(\tau) - Q(\tau'))$. However, there will also appear terms like $\dot{Q}^2(\tau) \cos \omega(Q(\tau) - Q(\tau'))$ and $\dot{Q}(\tau)\dot{Q}(\tau') \cos \omega(Q(\tau) - Q(\tau'))$ coming from the velocity-dependent terms in Eq. (4.3) to (4.8). We can rearrange $\dot{Q}(\tau)\dot{Q}(\tau')$ as $(\dot{Q}^2(\tau) + \dot{Q}^2(\tau') - (\dot{Q}(\tau) - \dot{Q}(\tau'))^2)/2$ which brings a constant shift in the domain mass and a dissipative term, which depends on the velocity of the wall. We then obtain an effective action that can be compared immediately with Eq. (3.3), coming from the Caldeira-Leggett model¹³ :

$$\begin{aligned} \Delta S_{eff}[Q, \dot{Q}] = & \frac{1}{2} \int_0^{1/T} d\tau \int_0^{1/T} d\tau' (Q(\tau) - Q(\tau'))^2 \alpha_L(\tau - \tau') \\ & + \frac{1}{2} \int_0^{1/T} d\tau \int_0^{1/T} d\tau' (\dot{Q}(\tau) - \dot{Q}(\tau'))^2 \alpha_T(\tau - \tau') - \frac{\tilde{M}}{2} \int_0^{1/T} \dot{Q}^2(\tau) \end{aligned} \quad (4.16)$$

where

$$\alpha_L = \frac{\pi}{4} \frac{S}{\rho} \frac{\lambda^4}{c_L^2} (A_{32} - A_{31})^2 \int_0^\infty d\omega \omega^5 \text{cosech}^2 \left(\frac{\pi \omega \lambda}{2 c_L} \right) D(\omega, |\tau - \tau'|) \quad (4.17)$$

$$\alpha_T = \frac{\pi}{16} \frac{S}{\rho} \frac{\lambda^4}{c_0^2 c_T^5} A_{44}^2 \int_0^\infty d\omega \omega^3 \text{cosech}^2 \left(\frac{\pi \omega \lambda}{2 c_T} \right) D(\omega, |\tau - \tau'|) \quad (4.18)$$

$$\tilde{M} = \frac{1}{3} \frac{S}{\rho_v} \frac{\lambda}{c_0^2} \left[\frac{1}{c_L^2} ((A_{32} - A_{31}) A_{33} - (A_{32} - A_{31})^2 / 2) + \frac{8}{c_T^2} A_{44}^2 \right] \quad (4.19)$$

This effective action is not completely equivalent to the Caldeira-Leggett action, due to the terms in \dot{Q} . This is of course a perfectly legitimate action, but its analysis is not simple. It however allows an easy identification of the dominant contribution to the dissipation. The normal dissipative term is of the superOhmic form ($J(\omega) \sim \omega^3$) as can be seen from Eq. (4.17). This is what would be expected from one-dimensional one-phonon processes⁷³. It must also be expected in the case of dissipation for a Bloch wall, since the wall restricts the phonon momentum in the plane of the wall to be zero (see Eq. (4.2)). The dissipative term coming from the coupling of the phonons to the velocity is described by a spectral function linear in ω , and looks at first sight to be of the Ohmic form. However, since it depends on the velocity of the wall, its effect is similar to superOhmic dissipation.

In the transverse kernel $\alpha_T(\tau - \tau')$, there appears the Walker velocity c_0 , defined in Eq. (2.5), and the transverse sound velocity whereas only the longitudinal sound velocity appears in $\alpha_L(\tau - \tau')$. In general, $c_0 < c_T < c_L$ so that depending on the value of the coefficient A_{44} , the term coming from the velocity of the wall might be the most important. Secondly, for a crystal of cubic symmetry, $A_{32} = A_{31}$ and dissipation comes only from the coupling between the phonons and the velocity of the wall. This can be traced back to our neglect of the influence of the coupling to the lattice in the determination of the shape of the wall. Taking it into account would give dissipation with a coefficient that would be smaller than the coefficient of the velocity-coupled dissipation by at least a factor of A_{ab}/C_{cd} , where C_{cd} are the elastic constants. For nickel, this is a reduction of $\sim 10^{-2}$, while for YIG it is $\sim 10^{-4}$, and it can be safely forgotten in both cases. This shows again that the coupling to the velocity of the wall is quite important. Let us then go back and perform the analysis by considering only the coupling between the phonons and the velocity of the wall.

C. 1-Phonon Coupling to the Wall Velocity

We now look exclusively at a wall with a cubic crystalline structure or with $c_0 < c_T$ such that the dominant mechanism for dissipation is from the coupling of the phonons to the velocity of the wall. As the wall is a one dimensional structure (in a flat wall approximation), one has the restriction $k_1 = k_2 = 0$. The only relevant terms in the magnetoelastic Lagrangian are thus

$$\begin{aligned} L_{int} = & \sum_{k_3} e^{ik_3 Q(\tau)} [A_{33} U_3(k_3, \tau) \mathcal{M}_3(-k_3) + A_{31} U_3(k_3, \tau) (\mathcal{M}_1(-k_3) + \mathcal{M}_2(-k_3)) \\ & + A_{44} U_4(k_3, \tau) \mathcal{M}_4(-k_3) + A_{55} U_5(k_3, \tau) \mathcal{M}_5(-k_3)] \end{aligned} \quad (4.20)$$

\mathcal{M}_3 and $\mathcal{M}_1 + \mathcal{M}_2$ are proportional to \dot{Q}^2 while \mathcal{M}_4 and \mathcal{M}_5 are proportional to \dot{Q} . We are considering exclusively tunneling of the wall so that the excursions in position can be restricted to second order in Q . This means that we can simply set $e^{ik \cdot Q} = 1$ in Eq. (4.20). Furthermore, the first three terms in Eq.(4.20) correspond to a renormalisation of the wall's mass; this is very small and we neglect it here. The two remaining terms contain a coupling of the phonons to \dot{Q} . However, $\mathcal{M}_5 \rightarrow 0$ as $k_3 \rightarrow 0$ while $\mathcal{M}_4 \rightarrow \pi\lambda$ in the same limit. Thus, the term in \mathcal{M}_5 gives rise to higher powers of $\omega = c_T k_3$ than \mathcal{M}_4 and it is sufficient to consider only the coupling to \mathcal{M}_4 . The effective coupling between the phonons and the wall is mediated by the Fourier transform of the strain tensor $U_4 = ik_3 u_2(k_3, \tau)$ (since $k_2 = 0$) and the effective interaction Lagrangian is

$$L_{int} = \dot{Q} \sum_{k_3} \tilde{C}_{k_3} u_2(k_3, \tau) \quad (4.21)$$

with the coupling constant

$$\tilde{C}_{k_3} = 4i\pi \frac{A_{44}}{2c_0} (k_3 \lambda)^3 \text{cosech}(\pi k_3 \lambda / 2) \quad (4.22)$$

Next, since the coupling is only to phonons in the x_2 direction, and with the restriction $k_1 = k_2 = 0$, we can use, as the new Lagrangian for the environment

$$L_{env} = \frac{1}{2} \sum_{k_3} \rho_v \dot{u}_2(k_3, \tau) \dot{u}_2(-k_3, \tau) + C_{44} k_3^2 u_2(k_3, \tau) u_2(-k_3, \tau) \quad (4.23)$$

The mapping to the Caldeira-Leggett oscillator bath is clearly $m_{k_3} = \rho_v / L_3$ and $\omega_{k_3} = c_T k_3 \equiv (C_{44} / \rho_v)^{1/2} |k_3|$. The way to treat this problem is now straightforward. A total time derivative first needs to be introduced, in order to change the coupling between the wall and the phonons from $\dot{Q} u_2$ to $Q \dot{u}_2$. This coupling to the velocity of the environment can then be eliminated by a canonical transformation on the environment^{13,32}. The resulting problem corresponds to a system coupled by its position to a new set of oscillators, with the same m_k and ω_k , but a new coupling constant $\tilde{C}_{k_3} = \omega_{k_3} \tilde{C}_{k_3}$ ³². The dissipative action is now in the usual Caldeira-Leggett form, with a spectral function

$$J_{\dot{Q}}^{(1ph)}(\omega) = \frac{\pi}{16} \frac{S_w}{\rho_v} \frac{\lambda^4}{c_0^2 c_T^5} A_{44}^2 \omega^5 \text{cosech}^2 \left(\frac{\pi \omega \lambda}{2 c_T} \right) \quad (4.24)$$

Thus the superOhmic $J(\omega) \sim \omega^3$ is recovered. This is the spectral function we shall use in the discussion of the dissipative effects of 1-phonon processes. We now turn to 2-phonon processes.

D. 2-Phonon Contributions to Action

Just as in the case of multiple magnons coupled to a domain wall^{3,5}, the extra phase space available for the interaction of pairs of phonons with a wall, means that 2-phonon couplings give a very different effect from 1-phonon couplings on the wall dynamics. To start with, the summation over the magnetoelastic indices in Eq. (4.12) is obviously more complicated. Let us first consider a static wall, so that $\mathcal{M}_1 = -\mathcal{M}_2$, $\mathcal{M}_3 = 0$, and let us use only the components $R_{111} = R_{222} = R_{333}$ of the second order magnetoelastic tensor. The summation is then

$$|\mathcal{M}_2|^2 [R_{ab1} R_{de1} - R_{ab1} R_{de2} - R_{ab2} R_{de1} + R_{ab2} R_{de2}] [\mathcal{G}_{ad}(\mathbf{k}, i\omega_n) \mathcal{G}_{be}(\mathbf{k}', i\omega_{n'}) + \mathcal{G}_{ae}(\mathbf{k}, i\omega_n) \mathcal{G}_{bd}(\mathbf{k}', i\omega_{n'})] \quad (4.25)$$

We use the fact that $c_T < c_L$, which allows us to keep only the term $G_T(p, i\omega_n)$ in Eq. (4.11) to simplify this expression to

$$|\mathcal{M}_2|^2 R_{111}^2 G_T(\mathbf{k}, i\omega_n) G_T(\mathbf{k}', i\omega_{n'}) [k_3^2 k_3'^2 (k_1^2 k_1'^2 + k_2^2 k_2'^2) + k_3^2 k_1'^2 k_2'^2 (k_1^2 + k_2^2) + k_3'^2 k_1^2 k_2^2 (k_1'^2 + k_2'^2)] \quad (4.26)$$

Secondly, one must be careful in performing the frequency summations. The two summations (over n and n') should be decomposed as summations over the sum and the difference of the frequencies, that is

$$T^2 \sum_{n=-\infty}^{\infty} \sum_{m=-\infty}^{\infty} \frac{1}{\omega_k^2 + \omega_n^2} \frac{1}{\omega_{k'}^2 + \omega_m^2} e^{i(\omega_n + \omega_m)(\tau - \tau')} = \\ -\frac{T}{2\omega_k \omega_{k'}} \sum_{r=-\infty}^{\infty} e^{i\omega_r(\tau - \tau')} \left([1 + n_B(\omega_k) + n_B(\omega_{k'})] \frac{\omega_k + \omega_{k'}}{\omega_r^2 + (\omega_k + \omega_{k'})^2} + [n_B(\omega_k) - n_B(\omega_{k'})] \frac{\omega_k - \omega_{k'}}{\omega_r^2 + (\omega_k - \omega_{k'})^2} \right) \quad (4.27)$$

where n_B is the boson occupation number,

$$n_B(\omega_k) = \frac{1}{e^{\omega_k/T} - 1} \quad (4.28)$$

By this separation, two different contributions can be identified. If we compare Eq. (4.27) with Eq. (3.7), it is clear that the wall can be considered to be coupled to two different oscillator baths. The first term on the right side of Eq.(4.27) corresponds to the simultaneous emission of two phonons followed by their re-absorption at a later time, while the second term corresponds to the scattering of two phonons off the wall. This latter process is not allowed for 1-phonon processes, due to energy-momentum conservation, but is perfectly possible once we consider 2-phonon processes. Of course, the scattering term requires phonons to be already present and is thus non-existent at $T = 0$ (we note that precisely the same discussion applies to magnons, for 2-magnon processes-involving a single bulk magnon- and 3-magnon processes, involving 2 bulk magnons^{3,5}; the only complication there was the necessity to include a single wall magnon as well). The emission/absorption term can be mapped to a Caldeira-Leggett environment provided that we identify $\omega \equiv \omega_k + \omega_{k'}$. The low energy behaviour, $\omega \rightarrow 0$ then comes from the limit $\omega_k, \omega_{k'} \rightarrow 0$, but looking back to Eq. (4.25), we see that this will implies superOhmic dissipation with a very high power in ω , due to the density of states of the phonons going to zero as $\omega_k \rightarrow 0$. This term can be completely ignored since it will always be much smaller than the 1-phonon contribution.

The scattering term however is very important as it represents Ohmic dissipation. The identification with a Caldeira-Leggett bath requires $\omega \equiv \omega_k - \omega_{k'}$, so that the low energy properties of the bath come from $\omega_k \rightarrow \omega_{k'}$. Now, nothing special happens to Eq. (4.25) in this limit, so the effective density of states for 2-phonon scattering processes is extremely reduced. The resulting dissipation is Ohmic, and although the numerical coefficient in front of it may be small, the fact that it is Ohmic means that it may be the dominant dissipative process, especially for coherent processes^{33,80}.

The temperature dependence of the friction coefficient is determined by the phonon density of states, and is thus different depending on the dimensionality of the phonons. We examine 1-, 2- and 3-dimensional phonons and concentrate on the scattering term, since the emission/absorption term results in superOhmic dissipation.

1. 3-Dimensional, 2-Phonon Processes

It is now straightforward to obtain the friction coefficient, although the calculations are somewhat complicated by the anisotropy of the problem. Keeping in mind the restrictions $k_1 + k'_1 = 0$ and $k_2 + k'_2 = 0$ coming from the form factor of the magnetisation, it is useful to perform the change of variables

$$\begin{aligned} \phi &= \tan^{-1} k_1/k_2 \\ \rho &= c_T(k_1^2 + k_2^2)^{1/2} \\ \omega &= c_T(k - k') = c_T \left[(k_3^2 + \rho^2)^{1/2} - (k'_3{}^2 + \rho^2)^{1/2} \right] \\ \epsilon &= c_T(k + k') = \frac{c_T}{2} \left[(k_3^2 + \rho^2)^{1/2} + (k'_3{}^2 + \rho^2)^{1/2} \right] \end{aligned} \quad (4.29)$$

After doing the angular integrals, the most important contribution to the effective action (the Ohmic one), can be isolated to give a dissipative action of the form

$$\Delta S_{eff}^{2ph} = \frac{T}{2\pi} \sum_n \int_0^{1/T} d\tau \int_0^{1/T} d\tau' \int_0^{\omega_D} d\omega \tilde{\eta}_{2ph}(Q(\tau) - Q(\tau'), \omega) e^{i\omega_n(\tau - \tau')} \frac{\omega}{\omega_n^2 + \omega^2} \sinh(\omega/2T) \quad (4.30)$$

where the cutoff is taken as the Debye frequency, defined by $\omega_D = c_T k_D$ with $k_D \sim 1/a_0$, the inverse of the lattice spacing. The detailed information of the dissipation is contained in the function $\tilde{\eta}_{2ph}(Q(\tau) - Q(\tau'), \omega)$. We are interested in the limit $\omega \rightarrow 0$ of the friction coefficient. After a further change of variables $x = \epsilon/T$ and $y = T^{-1}(\epsilon^2 - \rho^2)^{1/2}$ we obtain

$$\begin{aligned} \tilde{\eta}(Q(\tau) - Q(\tau'), 0) &= \left(\frac{R_{111}}{\rho_v c_T^2} \right)^2 \left(\frac{T}{c_T} \right)^4 \int_0^{\omega_D/T} dx \frac{1}{x^4 \sinh^2(x/2)} \\ &\int_0^x dy y \left(y^6 - \frac{3}{2} x^2 y^4 + \frac{1}{2} x^6 \right) \mathcal{M}_2^2(2yT/c_T) \cos[2yT(Q(\tau) - Q(\tau'))/c_T] \end{aligned} \quad (4.31)$$

Provided that $k_D(Q(\tau) - Q(\tau')) \ll 1$ it is possible to expand the cosine and keep only the quadratic term in Q . We are then in presence of conventional Ohmic Caldeira-Leggett dissipation. At temperature such that $T \ll \theta_D$, the Debye temperature defined as $k_B \Theta_D = \hbar \omega_D$, the dissipation is then characterised by the friction coefficient

$$\eta_{2ph}^{3d} = \frac{3}{5} \Gamma(7) \pi \hbar \left(\frac{R_{111}}{\rho_v c_T^2} \right)^2 S_w \lambda^2 \left(\frac{k_B T}{\hbar c_T} \right)^6 \quad (4.32)$$

where we have reinstated \hbar and k_B to get the correct units, S_w is the area of the wall and $\Gamma(x)$ is the Gamma-function. Alternatively, it can be written in term of the Debye temperature Θ_D as

$$\eta_{2ph}^{3d} = \frac{108}{5} \Gamma(7) \pi^5 \hbar \left(\frac{R_{111}}{\rho_v c_T^2} \right)^2 \frac{S_w \lambda^2}{a_0^6} \left(\frac{T}{\Theta_D} \right)^6 \quad (4.33)$$

where a_0 is the lattice spacing of the material. The numerical factor comes from taking $k_D^3 = 6\pi^2/a_0^3$. It shouldn't of course be taken too literally but nevertheless gives the right order of magnitude of the coefficient. Due to the presence of the temperature to the 6th power, we do not expect the 2-phonon processes to be relevant at really low temperatures, the question being of course: how low is sufficiently low! We will consider this question below.

Notice that we did not include any terms coupling the phonons to the velocity of the wall, as we did for 1-phonon processes. The reasons are twofold. First, it is clear that the fact that we obtain Ohmic dissipation coming from 2-phonon processes is not related in any way to the *form* of the coupling between the phonons and the magnetisation. Therefore, including the terms in \dot{Q} would only result in temperature dependent superOhmic dissipation, a process much weaker than the 1-phonon terms (remember that an apparent Ohmic dissipation in \dot{Q} corresponds effectively to superOhmic dissipation). Secondly, the component of the second order magnetoelastic tensor required for such a coupling would be of the form R_{555} and this is at least four orders of magnitude smaller than R_{111} (at least in bulk materials^{85,83}), and can be ignored.

2. 2-Dimensional Phonons and Néel Walls

Since the Néel wall is essentially a 1-dimensional structure, the analysis of 1-phonon dissipation in a thin film will be quite similar to the one in the bulk. The only difference is that there is now a large component of the magnetisation in the direction of the wall motion. The form factors of the Néel wall are thus

$$\begin{aligned} \mathcal{M}_1^{(N)} &= \mathcal{M}_1^{(B)} & \mathcal{M}_4^{(N)} &= \mathcal{M}_4^{(B)} \\ \mathcal{M}_3^{(N)} &\leftrightarrow \mathcal{M}_2^{(B)} & \mathcal{M}_5^{(N)} &\leftrightarrow \mathcal{M}_6^{(B)} \end{aligned} \quad (4.34)$$

Again the contribution to the effective action contains longitudinal terms, and transverse terms coming from the velocity of the wall. Due to the structure of a Néel wall, the longitudinal term is now proportional to $(A_{33} - A_{31})^2$, which is non-zero even in the case of a cubic structure. The transverse kernel, however, still contains the Walker velocity c_0 and we can assume that it still gives the dominant contribution to dissipation and can be used alone. The analysis of the Néel wall with a velocity-coupling to the phonons is exactly analogous to what was done for the Bloch wall, and the spectral function is completely equivalent to Eq.(4.24):

$$J_{\mathcal{N}}^{1ph}(\omega) = \frac{\pi}{16} \frac{A_w}{\rho_s} \frac{\lambda^4}{c_0^2 c_T^5} A_{44}^2 \omega^5 \text{cosech}^2 \left(\frac{\pi \omega \lambda}{2 c_T} \right) \quad (4.35)$$

where A_w is the cross-sectional area of the wall, ρ_s is the surface density and the constant A_{44} is in units of J/m².

The procedure for analysing 2-phonon processes is similar to the 3-dimensional case, but there are two differences. First, the density of states of the phonons is reduced and this will reduce the the power of the temperature in the friction coefficient. Secondly, the summation over the components of the magnetoelastic tensor is

$$|\mathcal{M}_3|^3 [R_{ab1} R_{de1} - R_{ab1} R_{de2} - R_{ab2} R_{de1} + R_{ab2} R_{de2}] [\mathcal{G}_{ad}(\mathbf{k}, i\omega_n) \mathcal{G}_{be}(\mathbf{k}', i\omega_{n'}) + \mathcal{G}_{ae}(\mathbf{k}, i\omega_n) \mathcal{G}_{bd}(\mathbf{k}', i\omega_{n'})] \quad (4.36)$$

If we assume $R_{111} = R_{222}$, then, due to the restriction $k_1 + k'_1 = 0$ coming from the δ -function of the magnetisation form factor, the whole summation is zero and there will be no dissipation coming from 2-phonon processes. However, there is no particular ground for such an assumption, as the second-order constants are almost unknown. In any case, if this is true, then one will certainly couple to the other components of the tensor, say R_{112} , R_{122} and so on. We will assume that such a coupling exists, so that we can write the friction coefficient for the motion of a domain wall as

$$\eta_{2ph}^{(2d)} \sim \Gamma(6)\hbar \left(\frac{\langle R \rangle}{\rho_s c_T^2} \right)^2 (A_w \lambda^2) \left(\frac{k_B T}{\hbar c_T} \right)^5 = \Gamma(6)(6\pi^2)^{5/3} \hbar \left(\frac{\langle R \rangle}{\rho_s c_T^2} \right)^2 \left(\frac{A_w \lambda^2}{a_0^5} \right) \left(\frac{T}{\Theta_D} \right)^5 \quad (4.37)$$

where both $\langle R \rangle$ and $\rho_s c_T^2$ are in units of Jm^{-2} .

3. 1-Dimensional Phonons in Magnetic Wires

The 1-dimensional case is also straightforward to treat. Only longitudinal phonons are present so the relevant components of the first- and second-order magnetoelastic tensors are A_{3a} and R_{33a} respectively. Without specifying the magnetisation profile, we simply assume that there exists an average interaction coupling $\langle A \rangle \lambda$ and $\sim \langle R \rangle \lambda$ between the wall and the phonons. The 1-phonon spectral function is then

$$J_{1ph}^{(1d)}(\omega) \sim \frac{1}{\rho_l} \frac{\lambda^4}{c_0^2 c_L^5} \langle A \rangle^2 \omega^5 \text{cosech}^2 \left(\frac{\pi \omega \lambda}{2 c_L} \right) \quad (4.38)$$

where we assumed that the dominant coupling was still to the velocity of the wall. In cases where such a coupling is not present, the Walker velocity c_0 should be replaced by the longitudinal sound velocity c_L . The 2-phonon processes still give rise to Ohmic dissipation, with a friction coefficient

$$\eta_{2ph}^{(1d)} \sim \Gamma(5)\hbar \left(\frac{\langle R \rangle}{\rho_l c_L^2} \right)^2 \lambda^2 \left(\frac{k_B T}{\hbar c_L} \right)^4 = \Gamma(5)(6\pi^2)^{4/3} \left(\frac{\langle R \rangle}{\rho_l c_L^2} \right)^2 \left(\frac{\lambda^2}{a_0^4} \right) \left(\frac{T}{\Theta_D} \right)^4 \quad (4.39)$$

with the expected reduction in the temperature dependence due to the reduction in the density of states.

E. Ohmic Coupling to Wall Chirality

The model of chirality tunneling, as proposed by Braun and Loss⁶¹ and Takagi and Tataro⁶⁰ was discussed in Section II. The models considered by these two groups are not completely equivalent. Braun and Loss consider a Néel wall in a wire while Takagi and Tataro use a Bloch wall. For definiteness, we concentrate on the Bloch wall model. The analysis can be trivially extended to a Néel wall.

In the model, the magnetisation components are defined as $(m_1, m_2, m_3) = (\cos \theta, \sin \theta \sin \phi, \sin \theta \cos \phi)$ with m_1 along the easy axis and m_3 normal to the plane of the wall. The angle $\theta = \theta(x_3 - Q)$ describes a Bloch wall with centre at a position Q along the x_3 -axis. However, the wall is pinned and the dynamical variable is $\phi(\tau)$, with a tunneling event corresponding to a transition from $\phi = \pm\pi/2$ to $\phi = \mp\pi/2$.

We now consider the effect of phonons on this chirality tunneling. The magnetoelastic interaction keeps the form in Eq. (3.18), but two points must be noticed:

- (i) The position of the wall is time-independent
- (ii) The form factors of the magnetisation are now explicitly time-dependent, through $\phi(\tau)$. The relevant form factors are

$$\mathcal{M}_2^B(\mathbf{q}) = -\frac{1}{2}(2\pi)^3 \delta(q_1) \delta(q_2) q_3 \lambda^2 \text{cosech}(\pi q_3 \lambda / 2) \sin^2 \phi(\tau) \quad (4.40)$$

$$\mathcal{M}_3^B(q_3, \tau) = \frac{1}{2}(2\pi)^3 \delta(q_1) \delta(q_2) q_3 \lambda^2 \text{cosech}(\pi q_3 \lambda / 2) \cos^2 \phi(\tau) \quad (4.41)$$

$$\mathcal{M}_4^B(q_3, \tau) = \frac{1}{2}(2\pi)^3 \delta(q_1) \delta(q_2) q_3 \lambda^2 \text{cosech}(\pi q_3 \lambda / 2) \cos \phi(\tau) \sin \phi(\tau) \quad (4.42)$$

We ignore \mathcal{M}_1^B , since it does not depend on the angle $\phi(\tau)$, and although \mathcal{M}_5^B and \mathcal{M}_6^B are non-zero, their effect is less important, since they go to zero as $q_3 \rightarrow 0$, as discussed in Section IV-A (cf. Eq. (4.9)). There are of course no terms depending on the velocity of the wall, and the 1-dimensional character of the Bloch wall still restricts the momentum of the phonons in the plane of the wall to be zero.

It is now straightforward to integrate out the phonon field and to obtain the dissipative action for the chirality

$$S_{eff} = \frac{\eta_{ab}^\chi}{4\pi} \int_0^{1/T} d\tau \int_0^{1/T} d\tau' T \sum_n \int_0^{\omega_D} d\omega e^{i\omega_n(\tau-\tau')} \frac{\omega^2}{\omega_n^2 + \omega^2} \Phi_a(\tau) \Phi_b(\tau) \quad (4.43)$$

with $\phi_0(\tau)$ contained in the functions $\Phi_a(\tau)$, with the values of a and b restricted to $a, b = 2, 3, 4$, and $\Phi_2 = \sin^2 \phi_0$, $\Phi_3 = \cos^2 \phi_0$ and $\Phi_4 = \cos \phi_0 \sin \phi_0$. This action is not a simple functional of the tunneling variable, but it is nevertheless clear that the dissipation is Ohmic, with a dimensionless coefficient $\alpha^\chi = \eta^\chi/\hbar$ given by

$$\alpha^\chi \sim \langle A \rangle^2 \frac{\lambda^2}{\rho_v} \frac{S_w}{\hbar c_L^3} \quad (4.44)$$

If we consider a wall of surface $S_w = S\text{\AA}^2$ in Ni ($\lambda \sim 500\text{\AA}$, $A_{ab} \sim 10^8 J/m^3$ and $c_L \sim 10^3 m/s$), then we obtain $\alpha^\chi \sim 10S$. Thus, even for a strictly 1-dimensional wall, in a sample with all nuclear spins removed, the coupling of 1-phonon processes to the chirality is obviously going to have a very severe effect on tunneling, and even more on coherence. We discuss how severe this effect is in the next section.

F. Remarks on Power-Counting

It is possible to explain the frequency dependence of the various spectral functions obtained in this section by some simple power counting arguments.

Let us start with 1-phonon processes. The spectral function describing the effect of isotropic acoustic phonons on the tunneling of defects or interstitials in an insulator is of the form $J(\omega) \sim \omega^{2+d}$ where d is the dimensionality of the system. This can be understood in the following way. The square of the matrix element coupling the phonons to the defect brings a power of ω . The coupling is through a term of the form $\exp(i\mathbf{k} \cdot \mathbf{q}(t))$ where k is the phonon's momentum and $q(t)$ is the position of the defect. Upon integration of the phonon field, this term results in a factor $\cos(|\mathbf{k} \cdot \mathbf{q}(t)|)$ (cf Eq. (4.17) and (4.18)) and it is clear that the expansion of the cosine to quadratic order in $(q(t) - q(t'))$ results in 2 more powers of $\omega = c|k|$ in the spectral function. Finally, the density of states of the phonons brings a factor ω^{d-1} .

With the magnetoelastic interaction, the matrix elements are the magnetoelastic constants, but since the interaction is through the strain tensor of the phonon field, this will also bring a power of ω to the spectral function. Thus, the spectral function of the phonons in a displacement tunneling situation is clearly the results of the uni-dimensional character of the Bloch wall, which reduces the effective density of states of the phonons from ω^{d-1} to ω , and this, independently of the physical dimension of the substrate.

Coming now to *chirality* tunneling, it is now obvious that the spectral function relating to the chirality tunneling should be Ohmic, since the phonons are effectively 1-dimensional, and there is no coupling of the form $\exp(ik \cdot \phi(t))$. Apart from numerical factors of $O(1)$, the different parameters entering the spectral function are understood easily from the spectral function of the phonons in a displacement tunneling situation simply by removing two powers of $k = \omega/c_L$ from Eq. (4.38) (and with the Walker velocity c_0 replaced by c_L).

The situation is more complex for 2-phonon processes. It was analysed in detail by Kagan and Prokof'ev⁸⁰ for the tunneling and diffusion of defects in insulators. In d dimensions, it was found that the Ohmic dissipation resulting from 2-phonon processes was described by a friction coefficient with temperature dependence $\eta(T) \sim T^{2+2d}$ (with "transport effects" included, as is appropriate for isotropic phonons). Again however, this is the result for a perfectly isotropic defect. A Bloch wall in a 3-dimensional material imposes $k_1 + k'_1 = k_2 + k'_2 = 0$; the problem is much more like the problem of magnons coupled to a wall^{3,5} (except that there one has the added problem of wall magnons). This then reduces the phonon density of states by a power of 2, which then results in the temperature dependence $\eta_{2ph}^{(3d)} \sim T^6$. In 2-dimensions, the only restriction is $k_1 + k'_1 = 0$, and as such only one power of the temperature will be missing with respect to the fully isotropic case, ie., $\eta_{2ph}^{(2d)} \sim T^5$. Finally, in 1 dimension, there is no lowering of the density of states due to the shape of the wall and we get $\eta_{2ph}^{(1d)} \sim T^4$.

Now that the dissipative effects of the phonons are known, we go on to examine the various dynamical processes of the wall.

V. TUNNELING OF DOMAIN WALLS COUPLED TO PHONONS AND NUCLEAR SPINS

We now come to the main practical results of the present paper. In sections III and IV we have seen that the main factors determining the tunneling dynamics of a domain wall at low T (for $kT < \Delta$, the magnon gap) will be (a) the

coupling to any defect or other pinning potential (b) the random hyperfine potential coming from nuclear spins, and (c) dissipation coming from both phonons and nuclear spins. In the present section, we will consider the case where the dissipative effects of nuclear spins are small (ie., $\lambda_I \ll 1$, cf. Eq. (3.33)). This will be the case for tunneling in wires of Ni or Fe (and compounds of these).

We are then left with the problem of a wall moving through a potential coming from both a pinning potential and the random hyperfine potential (recall the latter is not small even if $\lambda_I \ll 1$), with dissipation coming from phonons only. Although the random hyperfine potential varies slowly compared to the “bounce time” for tunneling processes, it still changes very quickly compared to any external field sweeps in an experiment.

At first glance the randomly-varying U_{hyp} appears to make a quantitative analysis of tunneling impossible. However, the situation is not so bad for Ni- and Fe-based materials, where the hyperfine coupling ω_0 is small, and the concentration x of nuclear spins is small. Even though $U_{hyp}(Q; \{\mathbf{I}_k\})$ may significantly perturb $V(Q)$, it varies sufficiently slowly in time that during a tunneling event, the total potential is essentially static. Since in any experimental run \tilde{V} is not necessarily known, the main effect of the $U_{hyp}(Q)$ is then be to renormalise \tilde{V} to a new value. A secondary effect is to slightly distort the barrier shape from a quadratic/cubic shape in a way which can be discussed quantitatively, for an ensemble of walls. This must be done in terms of Eq. (3.31), and corresponding higher moments. This kind of theory works best if the change ΔU in the potential caused by the hyperfine potential inside the wall satisfies $|\Delta U|/\tilde{V} \ll 1$. This is well-satisfied for most Fe- and Ni-based magnets. For rare earth magnets, $|\Delta U|/\tilde{V}$ may be very large indeed, and then an analysis using the quadratic/cubic approximation will be almost meaningless.

Even though $|\Delta U|/\tilde{V} \ll 1$ for Ni- and Fe-based systems, there are still rare large negative fluctuations of ΔU in time. If the external field is swept slowly, the wall can tunnel long before the “bare” pinning barrier is small. Thus the observed tunneling characteristics will depend on the sweep rate, and, at slow sweep rates, the wall will cross over “too early” to tunneling, from classical activation, and at too high a temperature.

A complete theory of the tunneling rate in this *dynamic* nuclear potential turns out to be extremely difficult; the solution of the dynamics in a *static* potential is difficult enough, even if one ignores tunneling⁸⁸. In the following we give an approximate theory, valid for slow sweep rates, and for short T_1 . Luckily these conditions are appropriate to the Ni experiments. This is described below; but first we discuss the tunneling in the complete absence of nuclear spins. The tunneling in this case is a simple problem of dissipative tunneling, entirely solvable with the results of section IV; we also use these results to look at chirality tunneling and “Bloch” tunneling of walls.

A. Wall Tunneling in Isotopically Purified Magnets

We first consider the problem of wall displacement tunneling, ie., the tunneling of the wall from some pinning centre, including the dissipative influence of the phonons on this tunneling. We then consider a system without any pinning centres (although possibly with more microscopic defects or impurities), and analyse the environmental influence on chirality tunneling and Bloch coherent tunneling.

1. Displacement Tunneling and Phonon Dissipation

When the defect potential is not perturbed by the nuclear spins, it is straightforward to obtain the corrections to the tunneling exponent due to dissipation, since dissipation is fairly weak. We find that the total tunneling exponent $B(T)$ is given by

$$B(T) = B_0 \left[1 + 15\alpha_t^{(d)}(T) + \frac{6}{\pi}\beta_t^{(d)} \left(1 - \left(\frac{T}{T_0} \right)^4 \right) \right] \quad (5.1)$$

where B_0 is the tunneling exponent in the absence of dissipation, given by Eq. (2.12). This expression includes the effects of both Ohmic and superOhmic dissipation, and is valid for walls in bulk, films and wires, through the dimensionality $d = 1, 2, 3$ of the phonons. It is valid up to terms of order $(T/T_0)^6$, provided that one is not too close to the “crossover region” between thermally activated and quantum barrier traversal^{73,74,76}. The dissipative processes entering in the effective action are shown schematically on Fig. (4). As stated earlier, we only consider the superOhmic dissipation coming from 1-phonon processes and the Ohmic dissipation coming from the scattering of a pair of phonons. To obtain the result (5.1), we first consider the bounce obtained in the absence of environment $Q(\tau) = Q_0 \text{sech}(\Omega_0\tau/2)$. Insertion of this solution into the effective action then yields the factor of $15\alpha_t^{(d)}(T) + (6/\pi)\beta_t^{(d)}$. The temperature corrections to the exponent are found in the usual way by an expansion of the bounce around its zero temperature form^{73,74,76}. Since the Ohmic dissipation due to 2-phonon processes is fairly weak and already strongly temperature

dependent, it is not necessary to calculate the temperature correction brought by it. Ohmic dissipation should be taken into account in the non-zero temperature form of the bounce which is used to calculate the temperature corrections due to 1-phonon processes but again, since the dissipation is weak, these can be calculated, in a first approximation, as if only 1-phonon processes were present. The calculation is standard and gives the factor $-(6/\pi^2)\beta_t^{(d)}(T/T_0)^4$. As usual, the effect of dissipation is smaller at non-zero temperatures.

Thus all phonon effects depend on the size of the two dimensionless parameters in (5.1). Ohmic dissipation comes from 2-phonon processes and the strength of this effect is parametrised by the dimensionless coefficient $\alpha_t^{(d)}(T) = \eta_{2ph}^{(d)}(T)/2M_w\Omega_0$, where M_w is the mass of the wall, Eq. (2.6), Ω_0 is the oscillation frequency of the wall in the potential well, Eq. (2.13) and $\eta_{2ph}^{(d)}$, the friction coefficient, is defined by the form of the spectral function $J(\omega) = \eta\omega$ and given by Eq. (4.39), (4.37) and (4.32) for 1-, 2- and 3-dimensional phonons respectively. Using the expressions for M_w and Ω_0 , we find

$$\alpha_t^{(d)}(T) = K_d \left(\frac{\langle R \rangle^{(d)}}{\langle C \rangle^{(d)}} \right)^2 \left(\frac{\lambda}{a_0} \right)^3 \left(\frac{M_0}{H_c} \right)^{1/2} \left(\frac{T}{\Theta_D} \right)^{3+d} \epsilon^{-1/4} \quad (5.2)$$

with $\epsilon = 1 - H/H_c$ defined by the external magnetic field and the coercive field, Eq.(2.9), and $\langle R \rangle^{(d)}$ and $\langle C \rangle^{(d)}$ are the relevant second order magnetoelastic constant and the elastic constant respectively. Thus $\langle R \rangle^{(d)}$ is in units of J/m^d , and $\langle C \rangle^{(d)} = \rho_d(c^{(d)})^2$, with $c^{(1)} = c_L$ and $c^{(d)} = c_T$ if $d = 2, 3$ and where ρ_d is the density appropriate to the dimensionality of the material. The constant K_d includes the numerical factors of the spectral functions Eq. (4.32), (4.37) and (4.39). For all practical purposes, we can take the order of magnitude estimate $K_d \sim 10^{2d+1}$. Notice that the power of the ratio between λ and a_0 is the same in all dimensions. This comes by using a wall of surface $S_w = a_0^2$ in $d = 1$ and $S_w = L_1 a_0$, with L_1 the cross-section of the wall in $d = 2$.

The usual 1-phonon processes give the expected superOhmic dissipation. We assume that the coupling between the phonons and the velocity of the wall gives the dominant contribution to the dissipation, so that the spectral function is given by Eq.(4.24). The strength of the dissipation is given by the dimensionless parameter $\beta_t = \tilde{\beta}\Omega_0/M_w$ (coming from $J(\omega) = \tilde{\beta}\omega^3$) and can be expressed as

$$\beta_t^{(d)} = \frac{1}{2\pi} \left(\frac{\langle A \rangle}{\langle C \rangle^{(d)}} \right) \left[\frac{\langle A \rangle \lambda \gamma_g}{c^{(d)} M_0} \right] \left(\frac{H_c}{M_0} \right)^{1/2} \epsilon^{1/4} \quad (5.3)$$

where $c^{(1)} = c_L$ and $c^{(d)} = c_T$ if $d = 2, 3$. Similarly, $\langle C \rangle^{(d)} = \rho_d c^{(d)}$, with ρ_d the density appropriate to the dimensionality of the material.

We can now analyse the general feature of Eq. (5.1). The salient feature is that there is a competition between 1-phonon and 2-phonon processes. The 1-phonon part of dissipation is stronger at $T = 0$ and decreases with increasing temperature while 2-phonon processes cause an increase in dissipation with the temperature. Of course, everything depends on the relative strength of the dimensionless couplings α_t and β_t . We now show that both β_t and α_t are quite small, with $\alpha_t < \beta_t$ in general.

Note first that α_t is strongly reduced by the factor $(T/\Theta_D)^{3+d}$, and to a lesser extent by the ratio of the second-order magnetoelastic constant to the elastic constant. This reduction is however offset by the numerical factor 10^{2d+1} , the ratio of the width of the wall to the lattice spacing and by the ratio between the magnetisation and the coercive field. Finally, there is a weak increase in dissipation as the height of the tunneling barrier is reduced. The total value will however be extremely small. Let us consider some parameters appropriate for Nickel (ie., $\lambda/a_0 \sim 10^2$ and $R/C \sim 10^{-1}$ and temperature such that $T/\Theta_D \sim 10^{-3}$). Then, we obtain $\alpha_t^d \sim 10^{-4-d}(M_0/H_c)^{1/2}\epsilon^{-1/4}$. Thus, even for very small coercive fields and very small tunneling barriers, the effect of 2-phonons processes can be neglected, and this even in wires. However, in the region of $T \sim 1K$, so that $T/\Theta_D \sim 10^{-2}$, the same estimate, in $d = 1$ gives $\alpha_t^{(1)} \sim 10^{-2}(M_0/H_c)^{1/2}\epsilon^{-1/4}$ and it is not obvious that such a term could be neglected. Since the experiments of Giordano are performed above 1 K, the question of the relevance of the 2-phonon term remains open.

The biggest contribution will thus come from the superOhmic dissipation caused by 1-phonon processes. This dissipation is independent of temperature, and decreases with decreasing coercive field and tunneling barrier height. Again, using the parameters of Nickel (with the first-order magnetoelastic constant $A \sim 10^8 J/m^3$), we obtain $\beta_t \sim (H_c/M_0)^{1/2}\epsilon^{1/4}$. The values of β_t should thus range between 0.01 – 0.1 in an experiment. This result also shows that the exact determination of H_c becomes quite relevant experimentally, as the value of β_t depends mostly on the ratio between H_c and M_0 (at least in this simple minded analysis for Nickel). In any case, even for a very strong coercive field, it is unlikely that β_t will become greater than 1 so that dissipation does not affect strongly the tunneling rate. The dependence of the tunneling rate on the temperature is certainly the most important effect arising from 1-phonon processes. In Fig. (5), we show the ratio $B(T)/B_0$ for a Bloch wall in a typical Nickel sample, using 3-dimensional phonons, which allow us to neglect 2-phonon processes.

Finally, in YIG, the magnetoelastic constants are a lot smaller ($A/C \sim 10^{-6}$ and $R/C \sim 10^{-4}$ and we do not expect any strong dissipative effect due to phonons, even in a temperature dependence of the tunneling rate.

2. Bloch tunneling and Chirality Tunneling?

So far we have considered only the simple process of the tunneling depinning from a defect potential. However, suppose that there are no such pinning potentials. What will then be the motion of the wall? One may consider one case, where, in absence of nuclear spins or dissipation, the wall would move quite freely (as in the case $\lambda \gg a_0$). Alternatively, one may consider a situation where a very thin wall, with $\lambda/a_0 \sim 1 - 10$, tunnels through a periodic lattice potential (a variant on this uses an artificially imposed periodic lattice potential, acting on a light wall having $\lambda/a_0 \gg 1$).

Let us first address the proposal that one might see coherent “Bloch band” motion of the walls in a periodic potential. Notice first just how restrictive the requirements are on such a process. One requires (a) almost perfect periodicity in the potential acting on the wall, such that deviations are much less than the bandwidth Δ_0 for translational tunneling (b) extremely weak dissipative effects from phonons or other bosonic environments, and (c) no possibility of any phase decoherence - by far the most serious source of which is environmental spins (topological decoherence).

The requirement of near perfect periodicity in the total static potential wall potential $V_W(Q)$ seems almost impossible to satisfy, at least in the foreseeable future. The basic problem is that the bandwidth Δ_0 will be extremely small, even for very small and light walls. Thus, Braun and Loss^{59,61} propose the example of a YIG wire with cross-section 100\AA , with a wall having $\lambda \sim 400\text{\AA}$; for this very light wall they estimate $\Delta_0 \sim 80mK$ (and a crossover to tunneling $T_0 \sim 50mK$). Thus, to satisfy the criterion of near periodicity in the potential, one requires that extrinsic corrections to $V_W(Q)$ (coming from non-uniformities in the wire cross-section, dislocations, defects, etc), be much smaller than $80mK$. However for this example the wall surface energy $\sim 10^{-4}J/m^2 \sim 7 \times 10^{18}K/m^2 \equiv 0.07K/\text{\AA}^2$, so this is a very tough requirement - the displacement of a single atom in the wire will cause a local change in $V_W(Q)$ considerably **larger** than Δ_0 !! In reality it is difficult at present to manufacture magnetic wires with better than a 5-10 per cent non-uniformity in wall cross-section, so that the fluctuations in the potential will be over energy scales some 3 orders of magnitude larger than this.

Thus the potential felt by the wall will realistically be like that shown in Fig. 6, with some very small periodic component superposed. Problems like this were considered in great detail in studies of the quantum diffusion of defects in solids (particularly muons).²⁷ The actual motion of the wall will be one of quantum diffusive motion between sites (eg., neighbouring potential wells), in which a thermal bath takes up the energy difference between sites (here via inelastic emission of phonon pairs, this being the dominant Ohmic process at low T).

Suppose that at $t = 0$ the wall is found in a potential well as shown on Fig. (6). Then, if δQ is the distance between this potential well and a nearby well with a lower minimum, the wall will tunnel at a rate given by quantum diffusion theory as²⁷

$$W = \frac{2(\Delta(\delta(Q)))^2 \Omega_{2ph}(T)}{\xi^2 + \Omega_{2ph}^2(T)} \frac{\xi/T}{1 - e^{\xi/T}} \quad (5.4)$$

with

$$\Omega_{2ph}(T) = T\eta_{2ph}(T)(\delta Q(\xi))^2/\hbar \quad (5.5)$$

where $\eta_{2ph}(T)$ is the 2-phonon Ohmic coupling calculated in section IV-C, and ξ is the energy difference between the bottom of the 2 wells; the tunneling matrix element $\Delta(\delta(Q))$ is that between the 2 wells (notice that $\Delta(\delta(Q))$ decreases exponentially as δQ increases, so that in most cases $\delta(Q)$ will be the distance between neighbouring potential wells of the periodic potential). Without more information about the nature of the background random potential, one cannot say much more here except that the wall will, at low T , move quantum diffusively towards the bottom of the nearest potential well of this potential.

Turning now to the possibility of chirality tunneling, one notes again the requirement that dissipation and decoherence be absent, as well as a complete energetic symmetry between the 2 chiral states. The requirement of energetic symmetry is still going to be extremely difficult to satisfy, and we also now have the very strong Ohmic coupling of single phonons to the chirality (Eq. (4.44)). From the example given after Eq. (4.44) we see that the dimensionless Ohmic coupling $\alpha_\chi \gg 1$ in almost all cases. This means, according to the standard results for Ohmic T -independent coupling,^{13,33} that (a) coherence will be suppressed completely (indeed the chirality variable will be *localized* at low T by the coupling to the phonons!), and (b) that the incoherent tunneling rate between the 2 chiralities will be suppressed by many orders of magnitude- so much so that we believe that for any reasonably-sized wall it can be

neglected (it is probably more to the point to ask why *thermally activated* transitions between chirality states has not been observed at higher temperatures).

This summarizes the results for an isotopically purified system. We see that the physics of wall displacement tunneling in an isotopically purified system is only weakly perturbed by phonons, in a way easily evaluated theoretically; thus it would be very interesting to see experiments performed in such ideal conditions. We expect the results to be very different in the presence of nuclear spins, as we now see.

B. Wall Tunneling in Dynamic Hyperfine field

We first analyse the tunneling for a Bloch wall; the results for a Néel wall are then obvious. The quasi-static potential experienced by the domain wall will be a sum of defect and random hyperfine fields:

$$V_W(Q) = V(Q) + U_{hyp}(Q; \{\mathbf{I}_k\}) \quad (5.6)$$

where $V(Q)$ is given by Eq. (2.7) and $U_{hyp}(Q; \{\mathbf{I}_k\})$ by Eq. (3.30). Over time scales Ω_0^{-1} , we see $U_{hyp}(Q; \{\mathbf{I}_k\})$ is indeed static.

In addition, the wall is coupled dynamically to phonons, via Eq. (3.16), and to the nuclear spins fluctuations, via (3.21).

At first glance it might seem that in systems like Ni, where the nuclear spins concentration $x \sim 0.01$, and $\omega_0 = 28.35$ MHz is very small, we might begin by ignoring the hyperfine field in favour of the “bare potential” $V(Q)$. Consider the ensemble averaged value of $\Delta U_{12} = C_{U_1 U_2}^{1/2}$ between points on either side of the tunneling barrier, here Q_1 is the entry point for tunneling and Q_2 is the exit point; recall (Eq. (2.14)) that $Q_1 - Q_2 = \lambda \epsilon^{1/2}$, in terms of $\epsilon = 1 - H_e/H_c$. We may estimate that

$$\frac{|\Delta U|}{\tilde{V}} = \frac{\omega_0 I}{\mu_0 \gamma_g H_c} \left(\frac{x}{N_0} \right)^{1/2} \epsilon^{-5/4} \quad (5.7)$$

where \tilde{V} is the barrier height at an applied field H_e (cf., Eq. (2.10)). For a Nickel wire, using the numbers in section II (cf., discussion following Eq. (2.15)), one finds that $|\Delta U|/\tilde{V} \sim 0.01$ only. Since in any experiment \tilde{V} is not known, the main effect of this small $U_{hyp}(Q)$ will be to simply renormalise \tilde{V} to a slightly different value, which is not directly observable, and which does not apparently change the physics very much (of course the same is not true for rare earth magnets, where we can easily verify the typically $|\Delta U|/\tilde{V} \gg 1$).

However even for Ni wires the above argument ignores the fact that if the applied field is static, or being swept only very slowly, then the actual tunneling of the wall can be controlled by the relatively rare but strong downward (ie., negative) temporal fluctuations in $U_{hyp}(Q; \{\mathbf{I}_k\})$ occurring in the tunneling barrier region.

A general treatment of this problem is beyond the scope of this paper. Here we will give an approximate treatment. Let us first consider the case of static external field (ie., zero sweeping rate), with some fixed small value of ϵ . In this case we shall define 3 characteristic time scales for the problem, viz.,

- (i) the tunneling traversal or bounce time Ω_0^{-1} , which will be very short (typically, $\Omega_0 > 10^9$ Hz).
- (ii) The characteristic time ${}^\perp T_{Diff}(\epsilon)$ for a fluctuation in the hyperfine field U_{hyp} to diffuse into or out of the barrier; since the barrier width is $\sim \lambda \epsilon^{1/2}$, we have

$${}^\perp T_{Diff}(\epsilon) \sim T_2 \frac{\lambda^2}{4a_0^2} \epsilon > T_2 \quad (5.8)$$

- (iii) Finally, the experimental tunneling time τ , ie., the inverse of the tunneling rate Γ at a given ϵ , in the presence of the fluctuating hyperfine potential; we shall estimate this below.

Let us consider the regime where

$$\Omega_0(\epsilon) \gg T_2 \quad (5.9)$$

$${}^\perp T_{Diff}(\epsilon) \gg \tau^{-1}(\epsilon) \quad (5.10)$$

The first inequality simply demands that the hyperfine potential be static during tunneling traversal - since $T_2^{-1} \sim 10^4 - 10^6$ Hz, this is always satisfied. The second inequality corresponds to the assumption that the wall always has enough time to sample enough tunneling paths (made available to it by fluctuations in U_{hyp} through the space of

possible potentials), that it will sample nearly “optimal” realisations of U_{hyp} (ie. those giving the maximum tunneling rate, or near to it). We shall see below when this assumption is consistent with our final answer for $\tau^{-1}(\epsilon)$. Once Eq. (5.9) and (5.10) are obeyed, we can estimate $\tau^{-1}(\epsilon)$ by functionally averaging over possible realisations of U_{hyp} , with a tunneling action appropriate to each, to get

$$\tau^{-1}(\epsilon) \sim \Omega_0(\epsilon) \int \mathcal{D}U(Q) \mathcal{P}(\{U(Q)\}) e^{-S(\{V_W(Q)\}, \dot{Q})} \quad (5.11)$$

where $\mathcal{P}(\{U(Q)\})$ is the probability for a particular realisation $U(Q)$ of the hyperfine potential to occur, and $S(\{V_W(Q)\}, \dot{Q})$ is the action for the tunneling trajectory through the total potential $V_W(Q) = V(Q) + U(Q)$ (cf., Eq. (3.30)). This equation makes no attempts to get pre-exponential factors right. Notice that Eq. (5.11) is independent of T_2 , because of condition (5.10). Thus the essential simplifying assumption in Eq. (5.11) is simply that if $\tau(\epsilon)$ is sufficiently long compared to ${}^{\perp}T_{Diff}(\epsilon)$, we do not have to worry about the “waiting time” required for $U(Q)$ to first approach an optimal realisation, everything boils down to the measure of such optimal configurations.

The assumptions Eq. (5.8) - (5.10) are probably satisfied in most wall tunneling problems. However, even with these assumptions, Eq. (5.11) is not easy to evaluate, it is a complicated path integral over different “paths” $U(Q)$ between Q_1 and Q_2 . We intend elsewhere to give a thorough analysis of (5.11). Here we shall estimate the change in $\tau(\epsilon)$ brought about by the fluctuating $U_{hyp}(Q)$ in the weak-coupling regime, where $|\Delta U|/\tilde{V}(\epsilon) \ll 1$, appropriate to Ni- and Fe-based systems, and show that the change is not important enough to explain the crossover temperature discrepancy reported by Giordano et al.

To make this estimate, we introduce a “typical” potential $U_\alpha(Q)$, having the form

$$U_\alpha(Q) \sim \alpha E_0 (Q/Q_0)^{1/2} \quad (5.12)$$

for $0 \leq Q \leq Q_0$, where the bare pinning potential $V(Q)$ has a minimum at $Q = Q_0$, and the tunneling end-point is at $Q = Q_0$. The value $\alpha = 1$ refers to the ensemble-averaged “gaussian half-width” value, ie., $E_0 = |\Delta U_{12}|$, so that

$$E_0 = \omega_0 s I N^{1/2}(\epsilon) \quad (5.13)$$

where $N(\epsilon) \sim N(\lambda)\epsilon^{1/2}$ is the number of nuclear spins swept by the wall in going from $Q = 0$ to $Q = Q_0$, and $N(\lambda) = x(S_w \lambda/a_0^3)$ as before. The ansatz Eq. (5.12) allows us to reduce (5.11) to a 1-dimensional integral:

$$\tau^{-1}(\epsilon) \sim \Omega_0(\epsilon) \int_{-\infty}^{\infty} \frac{d\alpha}{\sqrt{2\pi}} e^{-\alpha^2/2} \exp\left(-\frac{1}{\hbar} \int dQ (2M_w V_w^\alpha(Q))^{1/2}\right) \quad (5.14)$$

and where the total potential $V_w^\alpha(Q)$ is given by the sum of $V(Q)$ (evaluated in quadratic/cubic approximation) and $U_{hyp}(Q)$ (approximated by $U_\alpha(Q)$ in (5.12)), ie.,

$$V_w^\alpha(x) = \frac{27}{4} \tilde{V}(\epsilon) (x^2 - x^3) + \alpha E_0 |x|^{1/2} \quad (5.15)$$

where $x = Q/Q_0$.

Eq. (5.14) is a drastic simplification of (5.11), but it allows us to extract the exponent in the tunneling rate in the limit where $E_0 \ll \tilde{V}(\epsilon)$, so that the last term in $V_w^\alpha(Q)$ is a small perturbation. If we write the bare tunneling amplitude exponent $B_0(\epsilon) \sim (M_w \tilde{V}(\epsilon))^{1/2}$ (this is equivalent to Eq. (2.12) or Eq. (2.15), within a constant $\sim O(1)$), then we can write the exponential in (5.14) as $\exp[-B(\epsilon, \alpha)/\hbar]$, where

$$B(\epsilon, \alpha) = B_0(\epsilon) \left(1 + \left(\alpha \frac{E_0}{\tilde{V}(\epsilon)}\right)^{2/3} \text{sign } \alpha + \frac{3}{2} \alpha \frac{E_0}{\tilde{V}(\epsilon)} + O((\alpha E_0/\tilde{V})^x)\right) \quad (5.16)$$

where $x > 1$. For $E_0/\tilde{V}(\epsilon) \ll 1$, the second term in Eq. (5.16) dominates over the third one in the integration in (5.14). Doing this integral by steepest descents yields a new tunneling rate

$$\tilde{\Gamma} \sim \Gamma_0(\epsilon) e^{-\tilde{B}(\epsilon)} \quad (5.17)$$

$$\begin{aligned} \tilde{B}(\epsilon) &= B_0(\epsilon) - \Delta B(\epsilon) \\ &\sim B_0(\epsilon) - c(E_0/\tilde{V}(\epsilon)) B_0^{3/2}(\epsilon) \end{aligned} \quad (5.18)$$

where $\Gamma_0(\epsilon)$ is the bare tunneling rate (Eq. (2.12)), and $c = \sqrt{3/2} - 2/9 \sim 0.6$. Notice that whereas $B_0(\epsilon) \sim \epsilon^{5/4}$ (Eq. (2.15)), we have $\Delta B(\epsilon) \sim \epsilon^{3/8}$. The decrease in the relaxation time $\tau(\epsilon) \equiv \tilde{\Gamma}^{-1}(\epsilon)$ is entirely due to the occasional downward fluctuations in $U_{hyp}(Q)$. However, we emphasise that in the regime of validity of our estimation of $\Delta B(\epsilon)$, ie., for $E_0/\tilde{V}(\epsilon) \ll 1$, we expect $\Delta B(\epsilon)/B_0(\epsilon) \ll 1$ as well (for values of $\tilde{B}(\epsilon)$ corresponding to observable relaxation times). In particular, for Ni-based magnetic wires, we do not expect a large effect on $\tau(\epsilon)$.

This concludes our analysis of the influence of nuclear spins on wall tunneling. We conclude that in Ni- and Fe-based systems, their influence is fairly small. However, in rare earth systems, where $E_0/\tilde{V}(\epsilon) \gg 1$, it is clear that their effects on both tunneling and the classical wall dynamics will be very large, and will require a more sophisticated theory, starting from the effective interaction Hamiltonian derived in section III (Eq. (3.28) and (3.29)).

Finally, we note that the nuclear spins will also adversely affect any Bloch tunneling, since $U_{hyp}(Q)$ further disturbs any periodicity in the potential. For Ni- and Fe-based systems, this effect is certainly much smaller than that caused by disorder and non-uniformities in the wire cross-section; but for rare earth magnetic wires it could easily be larger.

VI. DISCUSSION: RELATION TO EXPERIMENTS

Let us now put together what we have learned from the results in sections III-V. With the assumption that for temperatures well below the magnon gap energy, the only significant environmental effects on domain wall tunneling can come from phonons and nuclear spins, we have set up a fairly complete theory for these effects in the limit where the nuclear spin effects are weak (the limit appropriate to Ni- and Fe-based magnets). We find that in this limit the phonon effects can be evaluated more or less exactly at these low energies, and involve 3 main effects - a superOhmic 1-phonon coupling to the wall velocity, a strongly T -dependent Ohmic coupling to the wall position (both of which are usually quite weak), and a very strong Ohmic 1-phonon coupling to the wall chirality. For a system isotopically purified of nuclear spins, these calculations suffice to determine completely the low- T tunneling behaviour; the “displacement tunneling” of the wall is weakly modified at finite T from that originally calculated by Stamp^{3,5}. On the other hand chirality tunneling is suppressed, and both it and “Bloch tunneling” seem to be practically unobservable, even for extremely small domain walls. Addition of nuclear spins makes the problem much harder, but for Ni- and Fe- based systems the effect of the dynamic fluctuating longitudinal hyperfine field on wall displacement tunneling is small enough that the change in the tunneling exponent can be estimated. One finds an increase in the tunneling rate over that expected without nuclear spins, caused by occasional strong negative fluctuations in the hyperfine potential.

The experimental implications for isotopically purified systems have already been discussed in section V.A. We summarize the key result in Fig. (5), which shows a typical T -dependence of the rate exponent for wall displacement tunneling from a pinning potential. It would be of some interest to test this result experimentally on, eg., an isotopically purified Ni magnetic wire, since the theory contains no adjustable parameters once the small oscillation frequency Ω_0 , the wall coercive field H_c , and the magnetostrictive constants are known.

For the case where the system contains naturally-occurring nuclear spins, a large number of experimental results exist already. The work by Giordano et al. on nominally single domain walls in Ni wires, includes (a) measurements of the tunneling rate Γ , at low T , and the quantum/classical crossover temperature T_0 , on various wires⁶ (b) measurements of the escape field statistics over a range of temperatures⁷, and (c) microwave measurements over a range of applied fields and temperatures, which give some evidence for level quantization of the trapped wall states⁸. In addition to these results there are many experiments on more complex wall systems, which give various kinds of evidence for tunneling^{10–12,52}. These experiments have been done at a variety of sweep rates, and for a wide variety of materials.

We may make a number of remarks concerning these results, on the basis of the present theory, as follows:

(i) *Quantum/Classical Crossover*: It is noticeable that some of these experiments show a crossover temperature T_0 considerably higher than the predicted^{5,3} value. In the experiments T_0 has usually been determined by looking for a low- T crossover to a plateau, in either the relaxation rate or the escape field; more sophisticated analyses look at the distribution of escape fields. One typically expects T_0 to *decrease* with increasing dissipative coupling to an oscillator bath, although how it does so, and the actual T -dependence of the transition rate, obviously depend on the nature of the bath (we are at a loss to explain why some experimentalists insist on using formulas appropriate to *Ohmic* baths to describe the crossover; this is never correct unless the low- T dissipation is dominated by electrons, which probably only happens for extremely thin walls, if at all). For isotopically purified systems it is clear from Fig. (5), that the simple estimate that $T_0 \sim (\Omega_0/2\pi)$, is reasonably accurate. However adding the nuclear spins makes the crossover much more complex. Suppose first the applied field is static (or being swept extremely slowly)- then the estimates in the previous section apply. We see immediately that for a given temperature, the distribution $P(H)$ of measured escape fields will be now be affected by both quantum/thermal fluctuations *and* by the fluctuations of $U_{hyp}(Q)$ in the barrier region, ie., there will be a T -independent extra spread in $P(H)$. A rough estimate of this extra spread is

obtained from the curvature of $B(\epsilon, \alpha)$ about its minimum in α ; this gives an extra spread $\sim E_0$ in bias ϵ , over and above the usual T -dependent quantum/thermal spreading^{7,89}.

This then suggests the enticing possibility that the anomalously high value found by Giordano et al., for T_0 in Ni wires, might be explained by the fluctuating U_{hyp} , which allows tunneling at a larger bias ϵ than in the absence of nuclear spins. However at the present time we do not think this is likely, simply because E_0 for this case is too small; as noted immediately following eq. (5.7), E_0 is roughly 2 orders of magnitude smaller than the typical barrier height.

(ii) *Resonant Absorption*: In the same way the microwave absorption results⁸ will have a linewidth which must be increased by $U_{hyp}(Q)$; the fluctuations in U_{hyp} will cause a fluctuation in the resonant frequency, again of order E_0 , and again T - independent. It is interesting to note that the linewidths in the Giordano-Hong experiments are rather large (much larger than one would expect from purely dissipative broadening), and in fact the linewidth is roughly what one would expect from the fluctuations in $U_{hyp}(Q)$ for these Ni wires. It would be useful to test this explanation of the line broadening. One obvious way is to redo the experiments on isotopically purified samples. The effect of the fluctuating $U_{hyp}(Q)$ should also be discernable as a low-frequency (of order $\sim^\perp T_{Diff}(\epsilon)$; cf eq. (5.8)) noise; ie., the resonant line is wandering at a frequency far lower than microwave frequencies (and far lower than the frequencies of thermal and quantum fluctuations). Similar problems are encountered in strongly non-linear optical systems, as well on experiments in glasses. We emphasize here that a full discussion of the effect of these dynamic hyperfine expressions on the experiments is premature; it requires the solution of the dynamics of the wall in a time-fluctuating, spatially random potential. As noted above, this problem is highly non-trivial, given the complexity of even the static problem⁸⁸. We regard its solution as an important problem- the fluctuating $U_{hyp}(Q)$ is so strong in rare earth magnets that it is clear that the domain wall motion will be strongly influenced by it, up to temperatures well above the hyperfine energy. At low T , the domain wall will be very strongly pinned by the $U_{hyp}(Q)$, so much so that the low frequency magnetic noise (Barkhausen noise) in the system will be completely determined by the time fluctuations in $U_{hyp}(Q)$. Our preliminary investigations of this question indicate that at low T , the wall motion will be dominated by "Levy flights", with a characteristic anomalous diffusion scaling behaviour predicted for the magnetic noise.

ACKNOWLEDGMENTS

We would like to acknowledge extremely useful discussions with N. Giordano, K. Hong, and N. V. Prokof'ev, and support from NSERC, the CIAR, and the UGF fund of the University of British Columbia.

-
- ¹ See the April 1995 issue of Physics Today, devoted to the subject of nanomagnetism.
- ² See the review of D. Gatteschi et al., Science **265**, 1054 (1994), of recent progress in making magnetic macromolecules.
- ³ P. C. E. Stamp, E. M. Chudnovski, B. Barbara, Int. J. Mod. Phys. **B 6**, 1355 (1992)
- ⁴ A fairly recent collection of articles on many aspects of tunneling in magnetic systems is in "*Quantum Tunneling of Magnetisation-QTM'94*", ed. L. Gunther, B.Barbara (Kluwer Publishing, 1995)
- ⁵ P. C .E. Stamp, Phys. Rev. Lett. **66**, 2802 (1991)
- ⁶ N. Giordano, J. D. Monnier, Physica **B 194-196**, 1009 (1994); K. Hong and N. Giordano, pp. 257-272 in ref. 4; K. Hong, N. Giordano, Phys. Rev. **B 51**,9855 (1995).
- ⁷ K. Hong, N. Giordano, J. Magn. Magn. Mat. **151**, 396 (1995); K. Hong and N. Giordano, J. Phys. CM **8**, L301 (1996).
- ⁸ K. Hong, N. Giordano, Europhys. Lett. **36**,147 (1996)
- ⁹ K. Hong, Ph.D. Thesis, Purdue University (Dec. 1995)
- ¹⁰ M. Uehara, B. Barbara, J. Physique **bf 47**, 235 (1986); M. Uehara, B. Barbara, B. Dieny, P. C. E. Stamp, Phys. Lett. **114A**, 23 (1986); B. Barbara, P .C. E. Stamp, M. Uehara, J de Physique **49**, C8-529 (1988)
- ¹¹ C. Paulsen et al., Phys. Lett. **161**, 319 (1991); C. Paulsen et al., Europhys. lett. **17**, 643 (1992).
- ¹² X. X. Zhang et al., Phys. lett. **A163**, 130 (1992); Ll. Balcells et al., Z. Phys. **B89**, 209 (1992).
- ¹³ A. O. Caldeira, A. J. Leggett, Ann. Phys. (N. Y.) **149**, 374 (1984)
- ¹⁴ R.F. Voss, R.A. Webb, Phys. Rev. Lett. **47**, 265 (1981)
- ¹⁵ S. Washburn, R.A. Webb, R.F. Voss, S.M. Faris, Phys. Rev. Lett. **54**, 2712 (1985)
- ¹⁶ A. N. Cleland, M. H. Devoret, J. Clarke, Phys. Rev. **B 36**, 58 (1987)
- ¹⁷ D. B. Schwartz, B. Sen, C. N. Archie, J. E. Lukens, Phys. Rev. Lett. **55**, 1547 (1985)
- ¹⁸ J. Clarke, A. N. Cleland, M.H. Devoret, D. Esteve, J. M. Martinis, Science **239**, 992 (1988)
- ¹⁹ R. Rouse, S. Han, J. E. Lukens, Phys. Rev. Lett. **75**, 1614 (1995); and S. Han, R. Rouse, J. E. Lukens, Phys. Rev. Lett. **76**, 3404 (1996)
- ²⁰ See, eg., C. M. Muirhead, W. F. Vinen, R. J. Donnelly, Phil. Trans. Roy. Soc. **A311**, 433 (1983), and refs. therein.

- ²¹ See, eg., H. J. Maris, J. Low Temp. Phys. **98**, 403 (1995); S. Balibar et al., J. Low Temp. Phys. **101**, 271 (1995); and H. J. Maris, Czech. J. Phys. **46**, supplement **S6**, 2943 (1996).
- ²² D. Bailin, A. Love, J. Phys. **A13**, L271 (1980)
- ²³ For tunneling in superconducting wires, see J.-M. Duan, Phys. Rev. Lett. **74**, 5128 (1995), and references therein.
- ²⁴ C. A. R. Sa de Melo, Phys. Rev. **B54**, 5829 (1996).
- ²⁵ J. Bardeen, Phys. Rev. Lett. **45**, 1978 (1980)
- ²⁶ A. F. Andreev, I. M. Lifshitz, J. E. T. P. **29**, 1107 (1969); B. V. Petukhov, V. L. Pokrovskii, J. E. T. P. **36**, 336 (1973).
- ²⁷ N. V. Prokof'ev, Y. Kagan, Chapter 2 in "Quantum Tunneling in Condensed Matter", ed. Y. Kagan, A. J. Leggett (Elsevier, 1992)
- ²⁸ N. V. Prokof'ev, Int. J. Mod. Phys. **B7**, 3327 (1993), and references therein.
- ²⁹ N. V. Prokof'ev, Phys. Rev. Lett. **74**, 2748 (1995).
- ³⁰ I. M. Lifshitz, Yu. M. Kagan, J. E. T. P. **35**, 206 (1972); S. V. Iordanskii, A. M. Finkelstein, J. E. T. P. **35**, 215 (1972).
- ³¹ M. B. Voloshin, I. Y. Kobzarev, L. B. Okun, Sov. J. Nucl. Phys. **20**, 644 (1975); S. Coleman, Phys. Rev. **D15**, 2929 (1977); C. Callan, S. Coleman, Phys. Rev. **D16**, 1762 (1977).
- ³² A. J. Leggett, Phys. Rev. **B 30**, 1208, (1984)
- ³³ A. J. Leggett et al., Rev. Mod. Phys. **59**, 1 (1987)
- ³⁴ A. J. Leggett, pp. 276-329 in "Frontiers and Borderlines in Many-Particle Physics", ed R.A. Broglia, J. R. Schrieffer (North-Holland, 1988).
- ³⁵ L. Weil, J. Phys. Chem. **51**, 715 (1954).
- ³⁶ C. P. Bean, J. D. Livingston, J. Appl. Phys. **30**, 1205 (1959)
- ³⁷ J. L. Van Hemmen, S. Suto, EuroPhys. Lett. **1**, 481 (1986)
- ³⁸ J. L. Van Hemmen, S. Suto, Physica **141 B**, 37 (1986)
- ³⁹ G. Scharf, W. F. Wreszinski, J. L. Van Hemmen, J. Phys. **20**, 4309 (1987).
- ⁴⁰ M.ENZ, R. Schilling, J. Phys. **C 19**, L711 (1986), and *ibid.*, 1765 (1986).
- ⁴¹ D. Loss, D. DiVincenzo, G. Grinstein, Phys. Rev. Lett. **69**, 3233 (1992).
- ⁴² J. von Delft, C. Henley, Phys. Rev. Lett. **69**, 3237 (1992); and Phys. Rev. **B48**, 965 (1993).
- ⁴³ N. V. Prokof'ev, P. C. E. Stamp, J. Phys. CM **5**, L663 (1993)
- ⁴⁴ P. C. E. Stamp, Physica **B 197**, 133 (1994)
- ⁴⁵ N. V. Prokof'ev, P. C. E. Stamp, pp. 347-371 in "Quantum Tunneling of Magnetisation -QTM '94", ed. L. Gunther, B. Barbara (Kluwer Publishing, 1995)
- ⁴⁶ N. V. Prokof'ev, P. C. E. Stamp, J. Low Temp. Phys. **104**, 143 (1996)
- ⁴⁷ N. V. Prokof'ev, P. C. E. Stamp, UBC preprint (April 1995), /cond-mat 9511011
- ⁴⁸ N. Abarenkova, J.C. Angles d'Auriac, Phys. Lett. **A219**, 335 (1996).
- ⁴⁹ A. Garg, M. Kim, Phys. Rev. **B43**, 712 (1991)
- ⁵⁰ L. Politi et al., Phys. Rev. Lett. **75**, 537 (1995); L. Politi et al., Int. J. Mod. Phys. **B10**, 2577 (1996).
- ⁵¹ For multi-grain experiments giving some evidence for tunneling, see, eg., F. Coppinger et al., Phys. Rev. Lett. **75**, 3513 (1995); J. Tejada, X. X. Zhang, J. Magn. Magn. Mat. **140-144**, 1815 (1995); B. Barbara et al., J. Magn. Magn. Mat. **140-144**, 1825 (1995); and references therein.
One should also note the *single grain* experiments of W. Wernsdorfer et al. (May 1997 preprint; see also W. Wernsdorfer et al., Phys. Rev. Lett. **78**, 1791 (1997)), which also see evidence for tunneling below 0.4K in $BaFe_{10.4}Co_{0.8}Ti_{0.8}O_{19}$ insulating nanoparticles.
- ⁵² For Multi-wall experiments giving some evidence for domain wall tunneling, see refs. 10-12, and also W. Wernsdorfer et al., Phys. Rev. **B53**, 3341 (1996), and *ibid.* **B 55**, 11552 (1997); or X. X. Zhang et al., J. Phys. CM **4**, L163 (1992), and Phys. Rev. **B53**, 3336 (1996).
- ⁵³ D. D. Awschalom, J. F. Smith, G. Grinstein, D. P. DiVincenzo, D. Loss, Phys. Rev. Lett. **68**, 3092 (1992); D. D. Awschalom et al., Science **258**, 414 (1992); S. Gider, D. D. Awschalom, pp. 243-255 in ref. 4 above; S. Gider et al., Science **268**, 77 (1995).
- ⁵⁴ The results of Awschalom et al. on ferritin molecules have been queried or criticised by a number of authors; questions have centered around the role of the dipolar coupling between molecules (ref.3 above); the experimental power absorption and lineshape, particularly in a field (see A. Garg, Phys. Rev. Lett. **70**, C2198 (1993), and reply of D. D. Awschalom et al., *ibid.*, C2199 (1993); or A. Garg, Phys. Rev. Lett. **71**, 4241 (1993), and the associated Comment of D. D. Awschalom et al., *ibid.*, C4276 (1993); or A. Garg, Science **272**, 425 (1996), with the reply of D. D. Awschalom et al., *ibid.*, 425 (1996)); the role of nuclear spins (see N. V. Prokof'ev and P. C. E. Stamp, refs. 45-47, and ref. 49 above), as well as A. Garg, Phys. Rev. Lett. **74**, 1458 (1995)); and finally the claimed inconsistency with high-T blocking (see J. Tejada, Science **272**, 424 (1996), and the reply by D. D. Awschalom et al., *ibid.*, 425 (1996)).
Note that in the later papers of Awschalom et al. it is found that the ferritin resonance frequency scales with the size of the Fe core roughly as one would expect from the coherent tunneling interpretation, which gives strong support to this explanation.
- ⁵⁵ Some of the recent Mn_{12} -acetate experiments include: C. Paulsen and J. G. Park, in ref. 3, pp 189-207 (1995); M. Novak and R. Sessoli, in ref. 3, pp 171-188 (1995); B. Barbara *et al.*, J. Magn. Magn. Mat., **140-144**, 1825 (1995); J. R. Friedman *et*

- al.*, Phys. Rev. Lett., **76**, 3830-3833 (1996); L. Thomas *et al.*, Nature **383**, 145-147 (1996). J. M. Hernandez *et al.*, Europhys. Lett., **35**, 301-306 (1996).
- See also the recent preprint by C. Sangregorio *et al.* (March 1997), which describes similar resonant tunneling in an Fe_8 molecular crystal.
- ⁵⁶ B. Leduc, MSc. Thesis, University of British-Columbia (1995); and to be published.
- ⁵⁷ G. Tatara, H. Fukuyama, J. Phys. Soc. Jap. **63**, 2538 (1994); G. Tatara, H. Fukuyama, Phys. Rev. Lett. **72**, 772 (1994)
- ⁵⁸ A. Wada, J. R. Schrieffer, Phys. Rev. **B 18**, 3897 (1978)
- ⁵⁹ H-B. Braun, D. Loss, J. Appl. Phys. **76**, 6177 (1994)
- ⁶⁰ G. Takagi, G. Tatara, Phys. Rev. **54**, 9920 (1996)
- ⁶¹ H-B. Braun, D. Loss, Phys. Rev. **B 53**, 3237 (1996)
- ⁶² A. P. Malozemoff and J. C. Slonczewski, "Magnetic Domain Walls in Bubble Materials" (Academic Press, 1979)
- ⁶³ L. D. Landau and E. M. Lifshitz, "Electrodynamics of Continuous Media" (Pergamon, London, 1975)
- ⁶⁴ M. V. Berry, Proc. R. Soc. Lond. A **392**, 45 (1987)
- ⁶⁵ *Geometric Phases in Physics* A. Shapere, F. Wilczek eds., World Scientific (1989)
- ⁶⁶ A. Auerbach, "Interacting Electrons and Quantum Magnetism", Springer-Verlag (1994)
- ⁶⁷ T. H. O'Dell, "Ferromagnetodynamics", MacMillan Press, (1981)
- ⁶⁸ E. M. Chudnovsky, O. Iglesias, P. C. E. Stamp, Phys. Rev. **B46**, 5392 (1992).
- ⁶⁹ L. Néel, Compt. Rend. Acad. Sci. Paris, **241**, 533 (1955).
- ⁷⁰ Aharoni, J. Magn. Magn. Mat. (1995 or 1996)
- ⁷¹ R. P. Feynman, F. L. Vernon Jr. , Ann. Phys. , (N. Y.) **24**, 118 (1963)
- ⁷² G.D. Mahan, "Many-Particle Physics", Plenum Press (1993)
- ⁷³ U. Weiss, "Quantum Dissipative Systems" (World Scientific, 1993)
- ⁷⁴ P. Hanggi, P. Talkner, M. Borkovec, Rev. Mod. Phys. **62**, 251 (1990)
- ⁷⁵ For the "Landau-Zener" model of the environment (which apparently goes back to the paper of D. L. Hill, J. A. Wheeler, Phys. Rev. **89**, 1102 (1953)), see, eg., the recent papers of A. Bulgac, G. Do Dang, D. Kusnezov, Phys. Rev. **E54**, 3468 (1996); Ann. Phys. **242**, 1 (1995); and E. Shimshoni, Y. Gefen, Ann. Phys. **210**, 16 (1991); and the many references therein.
- ⁷⁶ H. Grabert, P. Olschowski, U. Weiss, Phys. Rev. **B 36**, 1931 (1986)
- ⁷⁷ L. D. Landau and E. M. Lifshitz, "Theory of Elasticity" Pergamon, London, 1975
- ⁷⁸ E. du Trémolet de Lacheisserie, "Magnetostriction: Theory and Applications of Magnetoelasticity" (CRC Press, 1993)
- ⁷⁹ J. P. Mason, Phys. Rev. **82**, 715 (1951)
- ⁸⁰ Y. Kagan, N. V. Prokof'ev, Sov. Phys. J. E. T. P. **69**, 1250 (1989)
- ⁸¹ L. Néel, J. de Physique et Radium **15**, 225 (1954)
- ⁸² E. Callen, H. B. Callen, Phys. Rev. **139A**, 455 (1965)
- ⁸³ D. E. Eastman, Phys. Rev. **148**, 530 (1966)
- ⁸⁴ A. E. Clark, R. E. Stanley, J. Appl. Phys. **32** 1172
- ⁸⁵ E. du Trémolet de Lacheisserie, J. Rouchy, J. Magn. Magn. Mat. **28**, 77 (1982)
- ⁸⁶ R. C. O'Handley, S. W. Sun, J. Magn. Magn. Mater., **104- 107**, 1717 (1992)
- ⁸⁷ A. M. Stoneham, "Defects in Solids", Clarendon Press, Oxford (1975).
- ⁸⁸ J. P. Bouchaud, A. Comtet, A. Georges, P. Le Doussal, Ann. Phys. (N. Y.), **201**, 285 (1990)
- ⁸⁹ T.A.Fulton, L.N.Dunkleberger, Phys. Rev. **B9**, 4760 (1974).

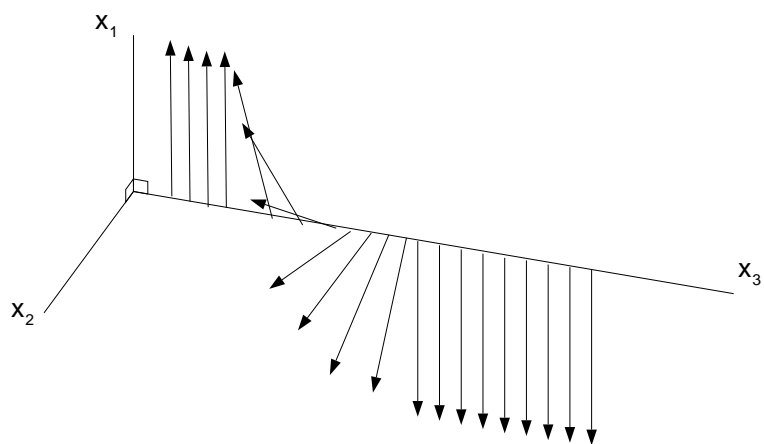


FIG. 1. The standard model of a Bloch Wall, with axes labelled as in the text.

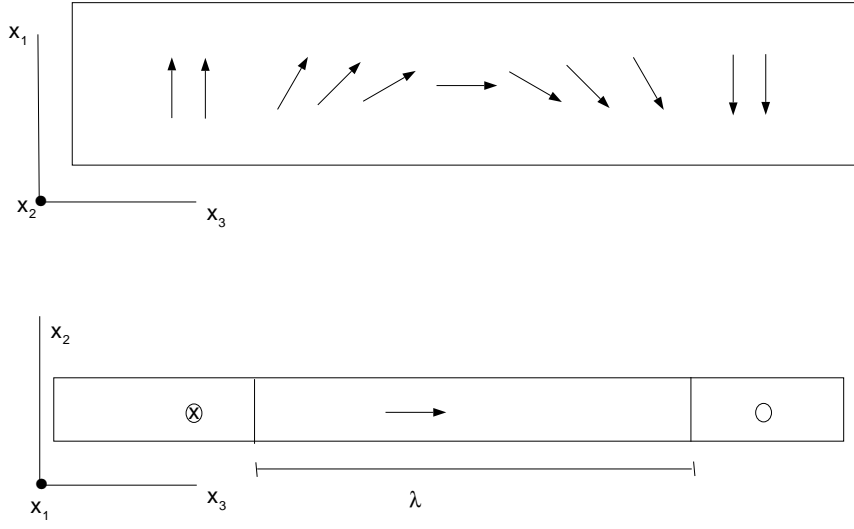


FIG. 2. The standard model of a Néel Wall, with axes labelled as in the text.

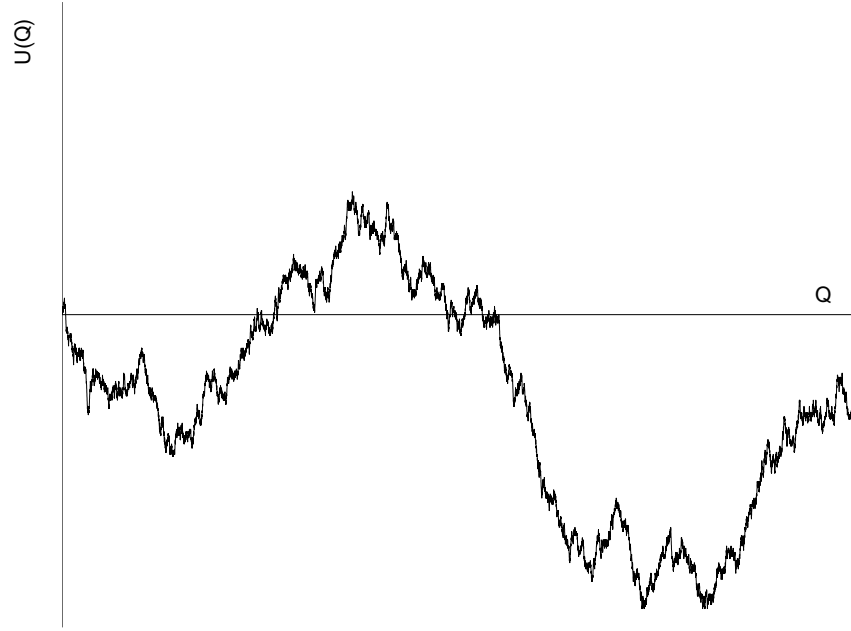


FIG. 3. Random potential caused by the nuclear spins when $kT \gg \omega_0$. At any given time the potential has a "random walk" form (the variance in spatial fluctuations of the potential increase as the square root of the distance travelled by the wall). The potential also slowly fluctuates in time, at a rate determined by nuclear spin diffusion.

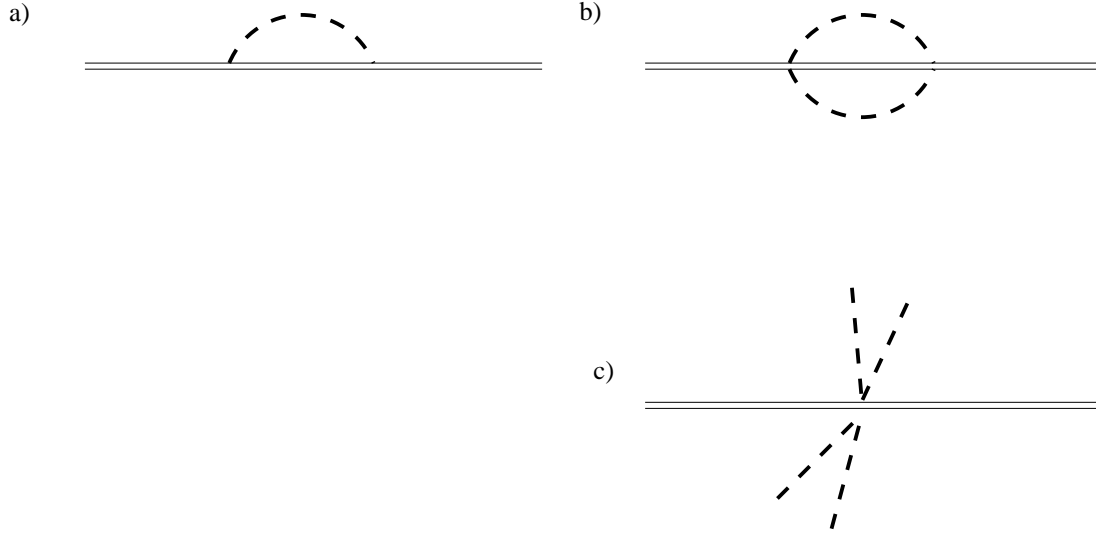


FIG. 4. Processes coming into the dissipative action of the domain wall. 3-a) represent the 1-phonon processes, 3-b) represents the simultaneous emission and reabsorption of 2 phonons and 3-c) is the scattering process giving rise to Ohmic dissipation

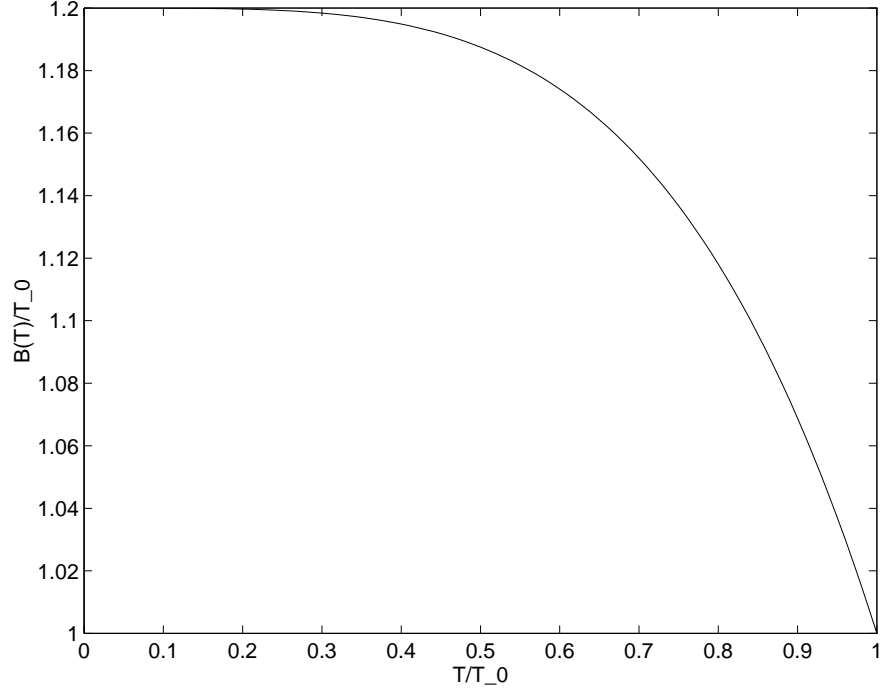


FIG. 5. Temperature dependence of the tunneling exponent $B(T)$, in the absence of nuclear spins. We show the result for 3-dimensional phonons, with 2-phonon processes being irrelevant, and assume a value $6\beta_t/\pi = 0.2$.

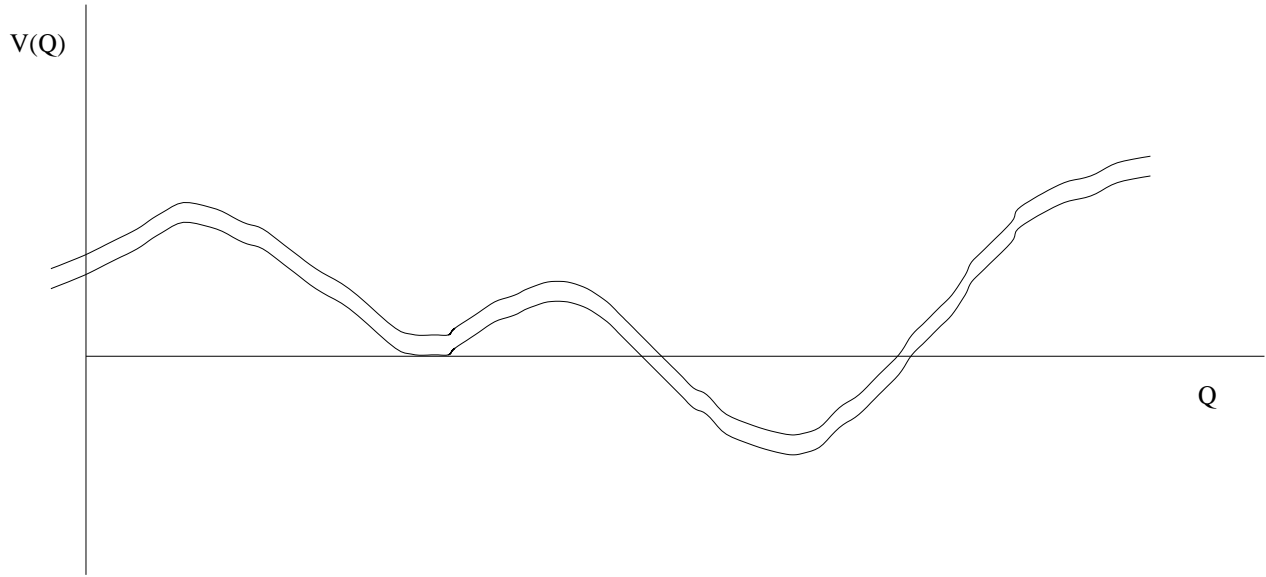


FIG. 6. Distortion of the putative Bloch band, caused by imperfections in the background periodic potential. This picture is meaningful if the variation caused by imperfections is over length scales long compared to the lattice spacing.